otic proteins, the multidomain proteins common in eukaryotes tend to fold incorrectly in the *E. coli* system, resulting in the formation of inclusion bodies.

Through decades of laborious work, scientists have identified three leading vaccine candidates from the pool of *P. falciparum* proteins: Pfs25 (19), PfCSP (5, 12, 34), and PfAMA1 (6, 11). Pfs25, a zygote/ookinete surface protein, is a promising candidate as a transmission-blocking vaccine. This protein is composed of four tandem epidermal growth factor-like domains, containing three putative N-linked glycosylation sites beside a signal peptide for the attachment of a glycosylphosphatidylinositol moiety (GPI anchor) at the C terminus. These characteristics render Pfs25 very difficult to express (18, 20). PfCSP, with its biased codon usage and lopsided amino acid composition, allows for only a minute amount of protein to be expressed in *E. coli* cells (34). The other antigen candidate is the PfAMA1 gene, which codes for a type 1 integral membrane protein of merozoites and is also difficult to express. Only a synthetic and codon-optimized gene has produced a fairly large amount of PfAMA1 protein in *E. coli* cells. Furthermore, a series of labor-intensive and technically complex refolding processes of the aggregates were required to use the protein as an antigen (6). The fact that only a few vaccine candidates are currently available (23) is most likely the result of difficulties in expressing malarial antigens in high quantity with their correct conformation.

We previously developed a wheat germ cell-free protein synthesis system for practical use in protein production. The system is especially powerful when used for the production of eukaryotic proteins because of its eukaryotic nature. We established two wheat germ cell-free protein protocols for practical use. The first can be used to produce a small amount of protein from a large number of cDNAs, in parallel, for the examination of product qualities and for the genome-wide biochemical annotation of gene products. In this approach, the templates for transcription are constructed using the split-PCR approach (29). The solution resulting from transcription is then directly used as the mRNA source in the small-scale bilayer translation system (28). The second protocol enables the production of large quantities of proteins. In this case, suitable gene products are first selected using the small-scale parallel production method and subsequent functional screening. Genes of interest are then cloned into the pEU plasmid (29), and the mRNA is transcribed. In the translational step, the protein production employs either the bilayer or the discontinuous batch translation method. The bilayer method has acceptable performance for the production of hundreds of micrograms of protein. Since 150 mg of a control protein in a reaction volume of 50 ml was produced in 5 h with the latter reaction method, the cell-free method can be scaled up (27). The system has been acknowledged in the fields of structural and functional genomics of eukaryotes (7, 32) and has proved advantageous due to its capacity to yield high-quality proteins. Taken together, the system seems to be powerful when used for the production of malaria parasite proteins, as no glycosylation takes place during the standard reaction. However, to date, there is no Good Manufacturing Practice facility for production of recombinant proteins for clinical studies using the wheat germ cell-free system in the world. In the present study, we first tested the versatility of the wheat germ cell-free system using as control models the leading vaccine candidate genes from *P. falciparum*. In addition, a series of experiments was conducted to prove the value of the system for the parallel expression of malaria proteins. The results presented here suggest that the wheat germ cell-free system may be useful as an additional protein production method in the field of *P. falciparum* research.

MATERIALS AND METHODS

Genomic cloning and construction of genes encoding fragments of Pfs25, PfCSP, and PfAMA1. The nucleotide sequences for the signal peptide and the GPI anchor were excluded from the expression constructs for genes encoding the PfCSP and Pfs25 proteins. The truncated versions of the PfCSP and Pfs25-3D7 genes were amplified by PCR from the genomic DNA of the *P. falciparum* 3D7 strain and subcloned into pEU3 (a vector carrying the C-terminal His_6 tag) (29) at the EcoRV site. The gene encoding Pfs25-TBV was a generous gift from Anthony W. Stowers (NIAID, NIH, Rockville, MD) (35). Pfs25-TBV, a synthetic version of the Pfs25 gene, was codon optimized for expression in the yeast *Saccharomyces cerevisiae*, and the replacement of Asn with Gln at three N-glycosylation sites was performed (20). DNA encoding full-length PfAMA1 protein was amplified from the genomic DNA of *P. falciparum* 3D7 and cloned into pEU-E01-GST (a vector with an N-terminal GST tag followed by a tobacco etch virus protease cleavage site) between the XhoI and BamHI sites. These pEU plasmid vectors are the expression vectors designed specifically for the wheat germ cell-free system (16). The inserted nucleotide sequences were confirmed using the ABI PRISM 310 Genetic Analyzer and the BigDye Terminator v1.1 Cycle Sequencing kit (Applied Biosystems, Foster City, CA).

Parallel construction of the DNA template from the parasite RNA. We selected 124 genes annotated as dominantly expressed in the blood stages of *P. falciparum* based on the microarray data integrated in the PlasmoDB database (http://www.plasmodb.org) (see Table S1 in the supplemental material). Extracted total RNA from *P. falciparum* 3D7 asexual blood-stage parasites was reverse transcribed into cDNA by using SuperScript III reverse transcriptase (Invitrogen, Carlsbad, CA), and PCR amplification was performed using *LA Taq* DNA polymerase (Takara Bio, Otsu, Japan). The 5′ primers were designed as 46-mers: 16-mer nucleotide sequences (5′-CCACCCACCACCACCA) as the S1 tag sequence followed by a 30-mer of unique sequence covering each 5′ open reading frame containing the start codon. For the 3′ primers, 30-mer nucleotide sequences covering each unique sequence upstream from the termination codon were prepared. The PCR products were then cloned into the pCR2.1 plasmid using a TOPO TA cloning kit (Invitrogen), and their sequences at both ends were confirmed. Translation templates were prepared by in vitro transcription from PCR products amplified by the split-primer PCR method described earlier (29).

Production and purification of the Pfs25-3D7/WG, Pfs25-TBV/WG, PfCSP/WG, and PfAMA1/WG proteins. We employed the wheat germ cell-free protein expression system for protein production using the bilayer translation reaction method described previously (28). Briefly, 250 μl of transcription mixture containing 25 μg of the plasmid DNA, 80 mM HEPES-KOH, pH 7.8, 16 mM magnesium acetate, 2 mM spermidine, 10 mM dithiothreitol, 2.5 mM each of nucleoside triphosphates, 250 U of SP6 RNA polymerase (Promega, Madison, WI), and 250 U of RNasin (Promega) was incubated for 6 h at 37°C. After the incubation, the transcription solution containing transcribed mRNA was mixed with 250 μl of wheat germ extract (60 A_{260} units) supplemented with 2 μl of 20-mg/ml creatine kinase in a single well of a six-well plate. The 5.5-ml substrate mix (30 mM HEPES-KOH, pH 7.8, 100 mM potassium acetate, 2.7 mM magnesium acetate, 0.4 mM spermidine, 2.5 mM dithiothreitol, 0.3 mM amino acid mix, 1.2 mM ATP, 0.25 mM GTP, and 16 mM creatine phosphate) from the ENDEXT Wheat Germ Expression S kit (CFS Co., Ltd., Matsuyama, Japan) was then added on top of the translation mix and incubated at 26°C for 12 h. After incubation, the reaction mixture was centrifuged at 21,900 × *g* for 20 min. Recovered supernatants were passed through Amicon Ultra centrifugal filter units (10-kDa molecular mass cutoff) (Millipore, Billerica, MA) to replace the translation buffer with phosphate-buffered saline. The samples containing the synthesized Pfs25-3D7/WG, Pfs25-TBV/WG, and PfCSP/WG proteins were purified using the Ni-nitrilotriacetic acid agarose column (Qiagen, Valencia, CA). The PfAMA1/WG protein was purified by passing the supernatant through the glutathione-Sepharose 4B column (GE Healthcare Bio-Sciences, Piscataway, NJ), followed by tobacco etch virus protease (Invitrogen) cleavage to remove the

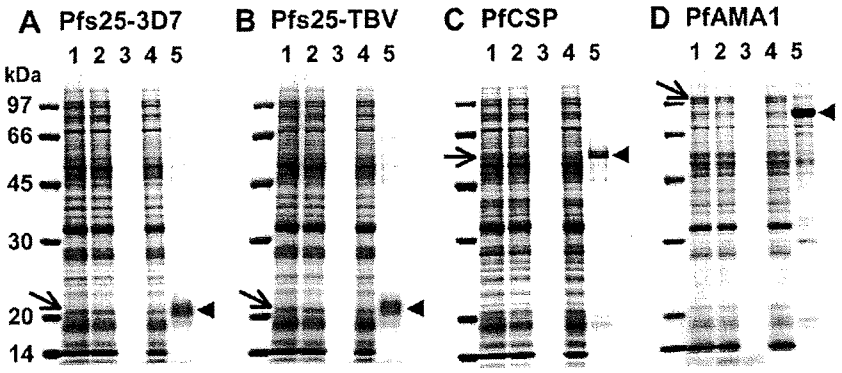

FIG. 1. SDS-PAGE analysis of the proteins expressed in the wheat germ cell-free system. Pfs25-3D7/WG (A), Pfs25-TBV/WG (B), PfCSP/WG (C), and PfAMA1/WG (D) were separated on SDS-12.5% polyacrylamide gels under reducing conditions and stained with Coomassie brilliant blue. The samples in each gel were as follows: total reaction mixture (lane 1), supernatant and precipitated fractions after brief centrifugation (lanes 2 and 3, respectively), and unbound and affinity-purified proteins (lanes 4 and 5, respectively). Products and purified proteins are indicated by arrows and arrowheads, respectively.

GST tag. Concentrations of affinity-purified proteins were determined using the Bradford protein assay kit (Bio-Rad Laboratories, Hercules, CA). Protein samples were separated by sodium dodecyl sulfate-polyacrylamide gel electrophoresis (SDS-PAGE) under reducing conditions (22), and the bands were visualized with Coomassie brilliant blue. Purified protein samples were stored in aliquots at −80°C until further use. For parallel protein synthesis from 124 malaria genes, the transcription and translation reactions were performed by a method similar to that described above. The 125-μl substrate mixture was overlaid on top of the 25-μl translation mixture containing transcribed mRNA in the presence of U-[^{14}C]Leu (11.1 kBq; 15 GBq/mmol of Leu). The reaction was performed in 96-well plates. Proteins were separated by SDS-PAGE and identified by autoradiography using an imaging analyzer (BAS-2500; Fujifilm, Tokyo, Japan). The solubility of each product was expressed as the percentage of trichloroacetic acid-insoluble radioactivity (counted using a liquid scintillation counter [LSC-6100; Aloka, Mitaka, Japan]) in a supernatant fraction recovered from centrifugation at 21,900 × *g* for 20 min compared to that of the total reaction mixture. The amount of target protein was estimated using the following formula where count is the radioactivity of the protein produced; Leu is the number of Leu residues in the protein, used to estimate the moles of Leu incorporated; MW is molecular weight; and ratio is the ratio of intensity of a specific protein band to the total intensity of bands on the autoradiogram: protein concentration = count/Leu × MW × ratio.

Preparation of antiserum. Groups of female BALB/c mice (five mice in each group) were subcutaneously immunized three times in the 1st, 3rd, and 5th weeks with 10 μg of affinity-purified proteins emulsified in Freund's adjuvant. As the control, a group of mice was administered GST in Freund's adjuvant, using the same protocol as described above. Antiserum preparation was as described elsewhere (2).

Preparation of *P. falciparum* asexual blood-stage parasites, ookinetes, and sporozoites. A mature schizont-rich fraction was obtained from cultured *P. falciparum* strain 3D7 (30). Parasite pellets were kept at −80°C until extract preparation.

To obtain ookinetes and sporozoites of *P. falciparum*, we used parasites derived from patient blood. The use of all human materials in this study was reviewed and approved by the Institutional Ethics Committee of the Thai Ministry of Public Health and the Human Subjects Research Review Board of the United States Army. Peripheral blood was collected with heparinized syringes under written informed consent from patients who came to the malaria clinics in the Mae Sod district, Thailand. Infection with *P. falciparum* was confirmed by the microscopic observation of Giemsa-stained thick and thin blood smears. The gametocytemic patient blood was divided into two parts. One was used to grow zygotes/ookinetes in vitro for both Western blotting and immunocytochemical analyses, and the other half was subjected to propagation of sporozoites in mosquitoes for two further analyses, as described elsewhere (33). Western blot analysis and immunocytochemistry were performed as described previously (3, 17).

Transmission-blocking assays. We collected 20 ml of peripheral blood from a volunteer patient. Blood was divided into aliquots (300 μl/tube) and briefly centrifuged, and plasma was discarded. Mouse immune sera against both Pfs25-3D7/WG and Pfs25-TBV/WG were serially diluted with heat-inactivated normal human serum prepared from malaria-naïve donors. Next, 180 μl of each diluted solution was added to the *P. falciparum*-infected blood cells and incubated for 15 min at room temperature. The mixture was placed in a membrane feeding apparatus kept at 37°C to allow *Anopheles dirus* A mosquitoes to feed on the blood in each apparatus for 30 min. Fully engorged mosquitoes were maintained for a week in the insectary. Oocysts that developed within the midgut were counted from 20 randomly selected mosquitoes. The Kruskal-Wallis test was applied to examine the differences in oocyst counts per mosquito between immunized groups and the control group fed on mouse serum raised against GST. Probability values (P) of less than 0.05 were considered statistically significant.

RESULTS AND DISCUSSION

We were able to successfully express the Pfs25/WGs, PfCSP/WG, and PfAMA1/WG proteins using the wheat germ cell-free system. Expression of the Pfs25 (Pfs25-3D7/WG) protein from a gene with a native nucleotide composition was shown by subsequent SDS-PAGE analysis (Fig. 1A) to be comparable in amount to that of Pfs25-TBV/WG (Fig. 1B) expressed from the codon-optimized synthetic gene. On the SDS-polyacrylamide gels, two protein bands appeared at 20 kDa, the expected mobility of the Pfs25 truncated form, lacking the signal peptide and the GPI anchor. Almost all of the Pfs25-3D7/WG protein from the biased DNA was recovered in the supernatant fraction (Fig. 1A, lane 2) and was easily purified as a single dominant band along with other nonspecific faint bands by affinity chromatography (Fig. 1A, lane 5). The amount of purified Pfs25-3D7/WG was 35 μg per 6.0 ml of the reaction mixture, while that obtained from the codon-optimized gene was comparable, at 30 μg protein per reaction mixture. These results demonstrate that the wheat germ cell-free system that we employed produced equal amounts of proteins with and without prior optimization of their biased codon usage in the DNA. Similarly, the amounts of the other two proteins, PfCSP/WG (Fig. 1C), and PfAMA1/WG (Fig. 1D), produced from a gene with a native nucleotide composition were 26 and 102 μg per reaction, respectively.

Immunological characterization of the protein products. To determine the creation of conformation-dependent epitopes in Pfs25 and AMA1, we examined and confirmed the reactivity of

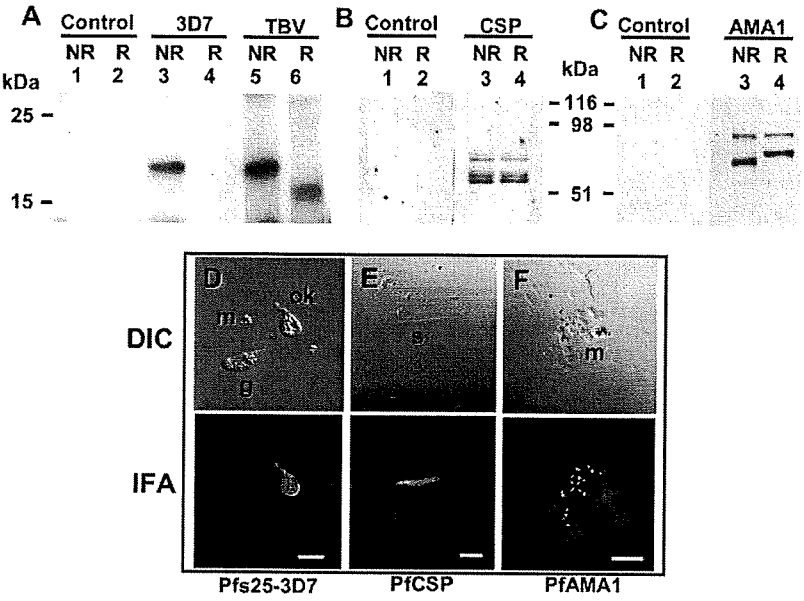

FIG. 2. Western blot and immunocytochemical analyses using antisera against Pfs25-3D7/WG, Pfs25-TBV/WG, PfCSP/WG, and PfAMA1/WG. Extracts prepared from *Plasmodium falciparum* zygotes/ookinetes (A), sporozoites (B), and schizonts (C) were separated on SDS-12.5% polyacrylamide gels under nonreducing (NR; lanes 1, 3, and 5) and reducing (R; lanes 2, 4, and 6) conditions. (A) Proteins on polyvinylidene fluoride membranes were immunostained either with mouse anti-Pfs25-3D7/WG serum (lanes 3 and 4) or mouse anti-Pfs25-TBV/WG serum (lanes 5 and 6) or with the negative-control serum (lanes 1 and 2). (B) The membrane was immunostained with either mouse anti-PfCSP/WG serum (lanes 3 and 4) or the control serum (lanes 1 and 2). (C) The membrane was immunostained with either mouse anti-PfAMA1/WG serum (lanes 3 and 4) or the control serum (lanes 1 and 2). (D to F) Samples prepared from *Plasmodium falciparum* immature ookinete (D), sporozoite (E), and schizont (F) were immunostained with the antiserum indicated at the bottom of the panel. Upper panels represent images obtained by differential interference contrast (DIC) microscopy, and lower panels represent immunostained images (immunofluorescence assay [IFA]) visualized with goat anti-mouse immunoglobulin G-fluorescein conjugate. These images have been taken by confocal scanning laser microscopy (LSM5 PASCAL; Carl Zeiss MicroImaging, Thornwood, NY). g, gametocyte; ok, immature ookinete; m, merozoite; s, sporozoite. Bars, 5 μm.

anti-Pfs25 conformation-specific monoclonal antibody 4B7 (a generous gift from Carole A. Long [NIAID, NIH, Rockville, MD]) against Pfs25/WGs and the reactivity of anti-PfAMA1 3D7 conformation-specific monoclonal antibody 1E9 (a generous gift from Carole A. Long) against PfAMA1/WG by Western blotting under nonreducing conditions (data not shown). To evaluate the immunogenicity of each protein prepared, we then raised mouse antisera and determined their reactivity to the parasite-derived native proteins. Extract from approximately 5×10^5 zygotes/ookinetes per lane was separated by SDS-PAGE, and Western blot analysis was performed. Specific bands with the expected mobility of native Pfs25 protein were detected under nonreducing conditions using antisera against Pfs25-3D7/WG and Pfs25-TBV/WG. Anti-Pfs25-3D7/WG serum did not show any reactivity under reducing conditions (Fig. 2A). These results suggest that the Pfs25-3D7/WG protein prepared here retained a conformation similar to that of the native protein. The identity of the faint band detected at the lower position with anti-Pfs25-TBV/WG under reducing conditions is unclear at present (Fig. 2A). Similar experiments were performed using anti-PfCSP/WG and anti-PfAMA1/WG sera to study extracts from respective stages of the parasite. The analyses clearly showed specific reactivity of each antiserum to PfCSP and PfAMA1 proteins (Fig. 2B and C). Anti-PfCSP serum reacted to three protein bands in the sporozoite extract under both reducing and nonreducing conditions (Fig. 2B). The upper and lower bands appeared to correspond to precursor and mature forms, respectively, as reported earlier by Coppi et al. (4). Anti-PfAMA1 serum gave two signals, with the upper and lower bands corresponding to mature and processed forms, respectively (15). The signal shift of the two bands upon introduction of a reducing reagent was most likely due to the high content of disulfide bonds within the protein (14). These results are consistent with previously reported findings (13).

Immunocytochemical staining was performed against immature ookinetes obtained by in vitro short-term culture using anti-Pfs25-3D7/WG. As shown in Fig. 2D (differential interference contrast and immunofluorescence assay), the antiserum specifically stained the surface of the immature ookinete but not the gametocyte and the merozoite. Antiserum against Pfs25-TBV/WG yielded similar results (data not shown). These findings were consistent with our previous report in which Pfs25-TBV prepared from yeast cells was used to raise antiserum (2). These findings also verified that Pfs25 prepared using our protocols from a gene with an A/T-rich native nucleotide composition can yield a protein of sufficient quality to raise a specific antibody. Experiments using anti-PfCSP/WG and anti-PfAMA1/WG on the target stages of the parasite showed typical staining patterns. The entire surface of the slender sporozoite was stained by anti-PfCSP/WG serum (Fig. 2E), and the anti-PfAMA1/WG serum clearly visualized punc-

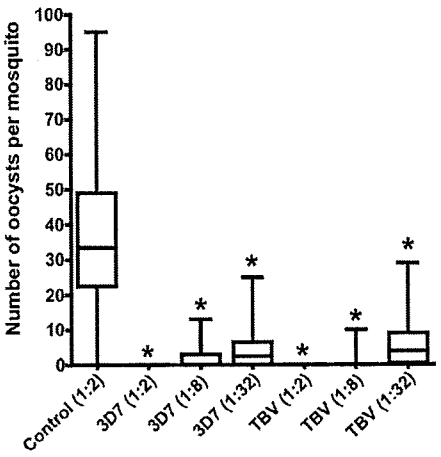

FIG. 3. Transmission-blocking efficacy of antibodies against *Plasmodium falciparum* parasites. The median numbers of oocysts per mosquito (n = 20) with quartiles (box plot) and ranges (lines on both top and bottom of the box) were compared among groups of mosquitoes fed on either anti-Pfs25 sera serially diluted or control mouse serum. Dilution of test immune serum is shown as 1:2 to 1:32. Statistical analysis was performed using the Kruskal-Wallis test for comparison of oocyst numbers between the test immune sera and control serum. Asterisks indicate statistically significant differences compared to the control group ($P < 0.05$).

tate localization of PfAMA1 at the apical end of merozoites (Fig. 2F).

Efficacy evaluation of the proteins as vaccine antigens. In view of a practical application of the system for discovery of malaria vaccine candidates, we evaluated the quality of antigens produced by performing a parasite growth inhibition assay using the antibodies raised against those antigens. We focused on Pfs25-3D7/WG and Pfs25-TBV/WG. Pfs25-TBV is currently the sole transmission-blocking vaccine candidate under clinical trial (23). A transmission-blocking assay was performed using both anti-Pf25-3D7/WG and anti-Pfs25-TBV/WG. A mixture containing *P. falciparum*-gametocyte infected erythrocytes and one of the antisera was fed to mosquitoes. The number of developed oocysts in the mosquitoes was then later counted. Both antisera at twofold dilution completely inhibited oocyst development, as we have seen no mosquito harboring oocysts (Fig. 3). The number of oocysts was inversely proportional to the concentration of antiserum added, findings consistent with previous experiments, in which Pfs25-TBV prepared from yeast was used to raise antiserum (2). It is important at this moment to stress the difference between this study and other studies: our proteins were produced from a non-codon-optimized gene in a cell-free system, while in other studies a codon-optimized engineered Pfs25-TBV gene was transformed into yeast cells (20). The results presented here strongly indicate the value of the wheat germ cell-free system for the production of malaria proteins that require complicated procedures in other systems.

Parallel syntheses of *P. falciparum* proteins. Although cell-based expression systems have been widely used in this field, they are limited mainly in their ability for efficient production of *P. falciparum* protein, primarily because of the complexity of the genome. In order to evaluate the capability of our cell-free system for parallel expression from the parasite genes, we selected 124 genes (see Table S1 in the supplemental material) encoding asexual blood-stage parasite proteins, based on the PlasmoDB database. Autoradiography demonstrated that 93 of the 124 genes yielded protein products. The average yield of expressed protein estimated for each full-size product was 1.9 μg per 150 μl of reaction mixture, an amount sufficient for preliminary antigen discovery studies using hyperimmune serum. Average protein solubility was 65% (see Table S1 in the supplemental material). There was significant inverse correlation between yield and molecular size of the protein; the greater the size, the lower the protein yield. There was also weak but significant inverse correlation between the protein yield and the relative frequency of low-complexity regions. In addition, solubility was inversely correlated with the pI value (Table 1). These observations have already been documented in earlier studies (24, 31). Surprisingly, we did not see any correlation between yield and A/T content, pI value, or the existence of a transmembrane domain (data not shown). We then analyzed the statistical difference in molecular weights, pI values, A/T contents, and relative frequencies of low-complexity regions between the expressed and nonexpressed groups of molecules, using the Mann-Whitney U test. The molecular weights in the nonexpressed group were significantly higher than those of the expressed group ($P < 0.0001$). In contrast, pI values, A/T contents, and the relative frequencies of low-complexity regions did not differ significantly (see Table S1 in the supplemental material). We currently have no explanation for why 25% of the tested genes failed to produce proteins in our system. One possible explanation is the sequence errors most likely present in the PCR products that were used as templates for transcription and subsequent translation. Such templates would cause mistranslation of the protein by frameshift.

In summary, the ability of the wheat germ cell-free protein synthesis system to produce *P. falciparum* proteins was examined. We found that (i) without the need for codon optimization, the cell-free system is able to produce a sufficient amount of high-quality proteins of the leading malaria vaccine candidates, Pfs25, PfCSP, and PfAMA1; (ii) biochemical, immunocytochemical, and biological analyses demonstrated that the prepared proteins could be directly used for immunization after a simple affinity purification step; and (iii) the system proved suitable for use as a parallel

TABLE 1. Correlation of expression or solubility and characteristics[a]

Parameter	Correlation coefficient (P value)	
	Protein concn	% Solubility
Mol wt	−0.3177 (0.0019)[b]	−0.1221 (0.2436)
pI	−0.1214 (0.2464)	−0.3519 (0.0005)[b]
% A/T	−0.1505 (0.1498)	
Low complexity[c]	−0.2276 (0.0283)[b]	
% Solubility	−0.0494 (0.6385)	

[a] Spearman's correlation coefficients by rank were calculated among the 93 proteins expressed. The probability values of the statistical significance are shown in parentheses.
[b] $P < 0.05$ was considered to indicate a statistically significant correlation.
[c] Relative frequency of low-complexity regions per molecular weight.

way to produce parasite proteins. We believe that the wheat germ cell-free protein synthesis system may be a key tool for decoding genetic information above and beyond malaria vaccine research.

ACKNOWLEDGMENTS

We thank Jeeraphat Sirichaisinthop and the staff of the Vector Borne Disease Training Center, Pra Budhabat, Saraburi, Thailand, for assistance in setting up the field sites and the staff of the Department of Entomology, AFRIMS, Bangkok, Thailand, as well as Hiroko Suzuki, Limei Yin, Kana Kato, and Aya Tamai for their technical assistance. We are grateful to Ivona Kozieradzki for critical reading of the manuscript and valuable comments.

This work was supported in part by Grants-in-Aid for Scientific Research (18390129 and 19406009) and Scientific Research on Priority Areas (19041053) from the Ministry of Education, Culture, Sports, Science and Technology of Japan and by a Grant-in-Aid from the Ministry of Health, Labor and Welfare (H17-Sinkou-ippan-019) of Japan.

REFERENCES

1. **Aguiar, J. C., J. LaBaer, P. L. Blair, V. Y. Shamailova, M. Koundinya, J. A. Russell, F. Huang, W. Mar, R. M. Anthony, A. Witney, S. R. Caruana, L. Brizuela, J. B. Sacci, Jr., S. L. Hoffman, and D. J. Carucci.** 2004. High-throughput generation of *P. falciparum* functional molecules by recombinational cloning. Genome Res. **14**:2076–2082.
2. **Arakawa, T., A. Komesu, H. Otsuki, J. Sattabongkot, R. Udomsangpetch, Y. Matsumoto, N. Tsuji, Y. Wu, M. Torii, and T. Tsuboi.** 2005. Nasal immunization with a malaria transmission-blocking vaccine candidate, Pfs25, induces complete protective immunity in mice against field isolates of *Plasmodium falciparum*. Infect. Immun. **73**:7375–7380.
3. **Arakawa, T., T. Tsuboi, A. Kishimoto, J. Sattabongkot, N. Suwanabun, T. Rungruang, Y. Matsumoto, N. Tsuji, H. Hisaeda, A. Stowers, I. Shimabukuro, Y. Sato, and M. Torii.** 2003. Serum antibodies induced by intranasal immunization of mice with *Plasmodium vivax* Pvs25 co-administered with cholera toxin completely block parasite transmission to mosquitoes. Vaccine **21**:3143–3148.
4. **Coppi, A., C. Pinzon-Ortiz, C. Hutter, and P. Sinnis.** 2005. The *Plasmodium* circumsporozoite protein is proteolytically processed during cell invasion. J. Exp. Med. **201**:27–33.
5. **Dame, J. B., J. L. Williams, T. F. McCutchan, J. L. Weber, R. A. Wirtz, W. T. Hockmeyer, W. L. Maloy, J. D. Haynes, I. Schneider, D. Roberts, et al.** 1984. Structure of the gene encoding the immunodominant surface antigen on the sporozoite of the human malaria parasite *Plasmodium falciparum*. Science **225**:593–599.
6. **Dutta, S., P. V. Lalitha, L. A. Ware, A. Barbosa, J. K. Moch, M. A. Vassell, B. B. Fileta, S. Kitov, N. Kolodny, D. G. Heppner, J. D. Haynes, and D. E. Lanar.** 2002. Purification, characterization, and immunogenicity of the refolded ectodomain of the *Plasmodium falciparum* apical membrane antigen 1 expressed in *Escherichia coli*. Infect. Immun. **70**:3101–3110.
7. **Endo, Y., and T. Sawasaki.** 2006. Cell-free expression systems for eukaryotic protein production. Curr. Opin. Biotechnol. **17**:373–380.
8. **Gardner, M. J., N. Hall, E. Fung, O. White, M. Berriman, R. W. Hyman, J. M. Carlton, A. Pain, K. E. Nelson, S. Bowman, I. T. Paulsen, K. James, J. A. Eisen, K. Rutherford, S. L. Salzberg, A. Craig, S. Kyes, M. S. Chan, V. Nene, S. J. Shallom, B. Suh, J. Peterson, S. Angiuoli, M. Pertea, J. Allen, J. Selengut, D. Haft, M. W. Mather, A. B. Vaidya, D. M. Martin, A. H. Fairlamb, M. J. Fraunholz, D. S. Roos, S. A. Ralph, G. I. McFadden, L. M. Cummings, G. M. Subramanian, C. Mungall, J. C. Venter, D. J. Carucci, S. L. Hoffman, C. Newbold, R. W. Davis, C. M. Fraser, and B. Barrell.** 2002. Genome sequence of the human malaria parasite *Plasmodium falciparum*. Nature **419**:498–511.
9. **Gowda, D. C., and E. A. Davidson.** 1999. Protein glycosylation in the malaria parasite. Parasitol. Today **15**:147–152.
10. **Greenwood, B., and T. Mutabingwa.** 2002. Malaria in 2002. Nature **415**:670–672.
11. **Gupta, A., T. Bai, V. Murphy, P. Strike, R. F. Anders, and A. H. Batchelor.** 2005. Refolding, purification, and crystallization of apical membrane antigen 1 from *Plasmodium falciparum*. Protein Expr. Purif. **41**:186–198.
12. **Heppner, D. G., Jr., K. E. Kester, C. F. Ockenhouse, N. Tornieporth, O. Ofori, J. A. Lyon, V. A. Stewart, P. Dubois, D. E. Lanar, U. Krzych, P. Moris, E. Angov, J. F. Cummings, A. Leach, B. T. Hall, S. Dutta, R. Schwenk, C. Hillier, A. Barbosa, L. A. Ware, L. Nair, C. A. Darko, M. R. Withers, B. Ogutu, M. E. Polhemus, M. Fukuda, S. Pichyangkul, M. Gettyacamin, C. Diggs, L. Soisson, J. Milman, M. C. Dubois, N. Garcon, K. Tucker, J. Wittes, C. V. Plowe, M. A. Thera, O. K. Duombo, M. G. Pau, J. Goudsmit, W. R. Ballou, and J. Cohen.** 2005. Towards an RTS, S-based, multi-stage, multi-antigen vaccine against falciparum malaria: progress at the Walter Reed Army Institute of Research. Vaccine **23**:2243–2250.
13. **Hodder, A. N., P. E. Crewther, and R. F. Anders.** 2001. Specificity of the protective antibody response to apical membrane antigen 1. Infect. Immun. **69**:3286–3294.
14. **Hodder, A. N., P. E. Crewther, M. L. Matthew, G. E. Reid, R. L. Moritz, R. J. Simpson, and R. F. Anders.** 1996. The disulfide bond structure of *Plasmodium* apical membrane antigen-1. J. Biol. Chem. **271**:29446–29452.
15. **Howell, S. A., C. Withers-Martinez, C. H. Kocken, A. W. Thomas, and M. J. Blackman.** 2001. Proteolytic processing and primary structure of *Plasmodium falciparum* apical membrane antigen-1. J. Biol. Chem. **276**:31311–31320.
16. **Kamura, N., T. Sawasaki, Y. Kasahara, K. Takai, and Y. Endo.** 2005. Selection of 5′-untranslated sequences that enhance initiation of translation in a cell-free protein synthesis system from wheat embryos. Bioorg. Med. Chem. Lett. **15**:5402–5406.
17. **Kaneko, O., B. Y. Y. Lim, H. Iriko, I. T. Ling, H. Otsuki, M. Grainger, T. Tsuboi, J. H. Adams, D. Mattei, A. A. Holder, and M. Torii.** 2005. Apical expression of three RhopH1/Clag proteins as components of the *Plasmodium falciparum* RhopH complex. Mol. Biochem. Parasitol. **143**:20–28.
18. **Kaslow, D. C., I. C. Bathurst, T. Lensen, T. Ponnudurai, P. J. Barr, and D. B. Keister.** 1994. *Saccharomyces cerevisiae* recombinant Pfs25 adsorbed to alum elicits antibodies that block transmission of *Plasmodium falciparum*. Infect. Immun. **62**:5576–5580.
19. **Kaslow, D. C., I. A. Quakyi, C. Syin, M. G. Raum, D. B. Keister, J. E. Coligan, T. F. McCutchan, and L. H. Miller.** 1988. A vaccine candidate from the sexual stage of human malaria that contains EGF-like domains. Nature **333**:74–76.
20. **Kaslow, D. C., and J. Shiloach.** 1994. Production, purification and immunogenicity of a malaria transmission-blocking vaccine candidate: TBV25H expressed in yeast and purified using nickel-NTA agarose. Biotechnology (New York) **12**:494–499.
21. **Kedees, M. H., N. Azzouz, P. Gerold, H. Shams-Eldin, J. Iqbal, V. Eckert, and R. T. Schwarz.** 2002. *Plasmodium falciparum*: glycosylation status of *Plasmodium falciparum* circumsporozoite protein expressed in the baculovirus system. Exp. Parasitol. **101**:64–68.
22. **Laemmli, U. K.** 1970. Cleavage of structural proteins during assembly of the head of bacteriophage T4. Nature **227**:680–685.
23. **Malkin, E., F. Dubovsky, and M. Moree.** 2006. Progress towards the development of malaria vaccines. Trends Parasitol. **22**:292–295.
24. **Mehlin, C., E. Boni, F. S. Buckner, L. Engel, T. Feist, M. H. Gelb, L. Haji, D. Kim, C. Liu, N. Mueller, P. J. Myler, J. T. Reddy, J. N. Sampson, E. Subramanian, W. C. Van Voorhis, E. Worthey, F. Zucker, and W. G. Hol.** 2006. Heterologous expression of proteins from *Plasmodium falciparum*: results from 1000 genes. Mol. Biochem. Parasitol. **148**:144–160.
25. **Richie, T. L., and A. Saul.** 2002. Progress and challenges for malaria vaccines. Nature **415**:694–701.
26. **Samuelson, J., S. Banerjee, P. Magnelli, J. Cui, D. J. Kelleher, R. Gilmore, and P. W. Robbins.** 2005. The diversity of dolichol-linked precursors to Asn-linked glycans likely results from secondary loss of sets of glycosyltransferases. Proc. Natl. Acad. Sci. USA **102**:1548–1553.
27. **Sawasaki, T., and Y. Endo.** 2008. The wheat germ cell-free protein synthesis system, p. 111–139. *In* A. S. Spirin and J. R. Swartz (ed.), Cell-free protein synthesis, methods and protocols. Wiley-VCH Verlag GmbH and Co. KGaA, Weinheim, Germany.
28. **Sawasaki, T., Y. Hasegawa, M. Tsuchimochi, N. Kamura, T. Ogasawara, T. Kuroita, and Y. Endo.** 2002. A bilayer cell-free protein synthesis system for high-throughput screening of gene products. FEBS Lett. **514**:102–105.
29. **Sawasaki, T., T. Ogasawara, R. Morishita, and Y. Endo.** 2002. A cell-free protein synthesis system for high-throughput proteomics. Proc. Natl. Acad. Sci. USA **99**:14652–14657.
30. **Trager, W., and J. B. Jensen.** 1976. Human malaria parasites in continuous culture. Science **193**:673–675.
31. **Vedadi, M., J. Lew, J. Artz, M. Amani, Y. Zhao, A. Dong, G. A. Wasney, M. Gao, T. Hills, S. Brokx, W. Qiu, S. Sharma, A. Diassiti, Z. Alam, M. Melone, A. Mulichak, A. Wernimont, J. Bray, P. Loppnau, O. Plotnikova, K. Newberry, E. Sundararajan, S. Houston, J. Walker, W. Tempel, A. Bochkarev, I. Kozieradzki, A. Edwards, C. Arrowsmith, D. Roos, K. Kain, and R. Hui.** 2007. Genome-scale protein expression and structural biology of *Plasmodium falciparum* and related Apicomplexan organisms. Mol. Biochem. Parasitol. **151**:100–110.
32. **Vinarov, D. A., B. L. Lytle, F. C. Peterson, E. M. Tyler, B. F. Volkman, and J. L. Markley.** 2004. Cell-free protein production and labeling protocol for NMR-based structural proteomics. Nat. Methods **1**:149–153.

33. **Wirtz, R. A., J. Sattabongkot, T. Hall, T. R. Burkot, and R. Rosenberg.** 1992. Development and evaluation of an enzyme-linked immunosorbent assay for *Plasmodium vivax*-VK247 sporozoites. J. Med. Entomol. **29:**854–857.
34. **Young, J. F., W. T. Hockmeyer, M. Gross, W. R. Ballou, R. A. Wirtz, J. H. Trosper, R. L. Beaudoin, M. R. Hollingdale, L. H. Miller, C. L. Diggs, and M. Rosenberg.** 1985. Expression of *Plasmodium falciparum* circumsporozoite proteins in *Escherichia coli* for potential use in a human malaria vaccine. Science **228:**958–962.
35. **Zou, L., A. P. Miles, J. Wang, and A. W. Stowers.** 2003. Expression of malaria transmission-blocking vaccine antigen Pfs25 in Pichia pastoris for use in human clinical trials. Vaccine **21:**1650–1657.

Editor: W. A. Petri, Jr.

BCA2/Rabring7 Promotes Tetherin-Dependent HIV-1 Restriction

Kei Miyakawa[1,2], Akihide Ryo[1]*, Tsutomu Murakami[1], Kenji Ohba[1], Shoji Yamaoka[2], Mitsunori Fukuda[3], John Guatelli[4], Naoki Yamamoto[1]*

1 AIDS Research Center, National Institute of Infectious Diseases, Shinjuku-ku, Tokyo, Japan, 2 Department of Molecular Virology, Graduate School of Medicine, Tokyo Medical and Dental University, Bunkyo-ku, Tokyo, Japan, 3 Department of Developmental Biology and Neurosciences, Graduate School of Life Sciences, Tohoku University, Sendai, Miyagi, Japan, 4 Department of Medicine, University of California San Diego, La Jolla, California, United States of America

Abstract

Host cell factors can either positively or negatively regulate the assembly and egress of HIV-1 particles from infected cells. Recent reports have identified a previously uncharacterized transmembrane protein, tetherin/CD317/BST-2, as a crucial host restriction factor that acts during a late budding step in HIV-1 replication by inhibiting viral particle release. Although tetherin has been shown to promote the retention of nascent viral particles on the host cell surface, the precise molecular mechanisms that occur during and after these tethering events remain largely unknown. We here report that a RING-type E3 ubiquitin ligase, BCA2 (Breast cancer-associated gene 2; also called Rabring7, ZNF364 or RNF115), is a novel tetherin-interacting host protein that facilitates the restriction of HIV-1 particle production in tetherin-positive cells. The expression of human BCA2 in "tetherin-positive" HeLa, but not in "tetherin-negative" HOS cells, resulted in a strong restriction of HIV-1 particle production. Upon the expression of tetherin in HOS cells, BCA2 was capable of inhibiting viral particle production as in HeLa cells. The targeted depletion of endogenous BCA2 by RNA interference (RNAi) in HeLa cells reduced the intracellular accumulation of viral particles, which were nevertheless retained on the plasma membrane. BCA2 was also found to facilitate the internalization of HIV-1 virions into $CD63^+$ intracellular vesicles leading to their lysosomal degradation. These results indicate that BCA2 accelerates the internalization and degradation of viral particles following their tethering to the cell surface and is a co-factor or enhancer for the tetherin-dependent restriction of HIV-1 release from infected cells.

Citation: Miyakawa K, Ryo A, Murakami T, Ohba K, Yamaoka S, et al. (2009) BCA2/Rabring7 Promotes Tetherin-Dependent HIV-1 Restriction. PLoS Pathog 5(12): e1000700. doi:10.1371/journal.ppat.1000700

Editor: Jeremy Luban, University of Geneva, Switzerland

Received April 21, 2009; **Accepted** November 18, 2009; **Published** December 18, 2009

Funding: This work was supported by grants from the IMAI Memorial Trust for AIDS Research, the Japanese Ministries of Education, Culture, Sports, Science and Technology (20390136, 13226027, 14406009 and 1941075), Health, Labour and Welfare (H18–005) and Human Health Science (H19–001) to AR and NY, and from the NIH USA (AI081668) to JG. The funders had no role in study design, data collection and analysis, decision to publish, or preparation of the manuscript.

Competing Interests: The authors have declared that no competing interests exist.

* E-mail: aryo@nih.go.jp (AR); nyama@nih.go.jp (NY)

Introduction

The human immunodeficiency virus (HIV) exploits the host cell machinery to maximize viral particle production [1]. In contrast, there are multiple systems in host cells that render them resistant to viral infection through the actions of innate host cell restriction factors [2,3]. This intracellular innate system can in turn be antagonized by certain viral proteins, creating a conflict between host cells and pathogens. There is accumulating evidence to now suggest that the balance between host and viral factors influences the susceptibility of the host cells to HIV infection and ultimately AIDS progression [4].

A human transmembrane protein, tetherin (also known as BST-2, CD317 or HM1.24) has been identified as an interferon-induced antiviral host factor in HIV-1-infected cells. During the late phase of the viral replication pathway, tetherin retains nascent HIV-1 virions at the plasma membrane and prevents viral spread [5 7]. Tetherin has been shown not only to block the release of lentiviruses such as HIV-1 or SIV, but also other viruses such as MLV, HTLV-1, Lassa virus and the Marburg virus [8 10]. These results indicate that tetherin has broad antiviral properties through the inhibition of viral particle release, and therefore that the activation of this protein might be an effective strategy as an anti-viral therapy.

Viral Protein U (Vpu) is a 16 kD phosphoprotein that is encoded almost exclusively by SIV_{CPZ} and its descendants, including HIV-1 [11–13]. Vpu is a factor that facilitates viral particle release by antagonizing tetherin-mediated viral restriction [6,7,14,15], in addition to its effects upon CD4 degradation [16 18]. The expression of Vpu has been shown to downregulate the tetherin levels on the plasma membrane resulting in effective virion release [7,19]. Indeed, Vpu-defective HIV-1 virions are efficiently retained on the plasma membrane and fewer viral particles are released compared with wild-type virions in tetherin-positive cells, including T cells and macrophages. [14,20]. On the other hand, in tetherin-negative cells, viral particle release is much less affected by either the presence or absence of Vpu [6,7]. These results suggest that Vpu antagonizes the function of tetherin, which otherwise restricts the release of HIV-1 from infected host cells. Following cell surface tethering, HIV-1 virions are subjected to internalization into CD63-positive endosomal compartments, thereby limiting the extent of virus spread [6,15,21 25]. Although tetherin can hold nascent viral particles on the cell surface of the host cells, the precise molecular events following the virion

Author Summary

Human cells possess multiple systems that render them resistant to viral infection. Recently, a transmembrane protein, tetherin, has been identified as an antiviral host factor in HIV-1-infected cells. Tetherin retains newly assembled virions at the plasma membrane and prevents viral release from the infected cells. However, the precise molecular mechanisms following the virion tethering remain largely unknown. In our current study, we have identified a RING-type E3 ubiquitin ligase, BCA2, which co-localizes and interacts with tetherin in human cells. BCA2 was found to facilitate the internalization of HIV-1 particles captured by tetherin on the plasma membrane and to enhance the targeting of viral particles to the lysosomes. Conversely, the targeted depletion of endogenous BCA2 reduces the intracellular accumulation of viral particles. Additionally, the expression of a small viral protein Vpu, an antagonist of tetherin, counteracts the antiviral effects of BCA2. These results suggest that BCA2 is a potential antiviral factor that collaborates with tetherin to facilitate the degradation of nascent HIV-1 particles during "post-tethering" processes.

tethering and identity of the related host factors that regulate these processes remain largely unknown.

In our current study, we identify a RING-type E3 ubiquitin ligase, BCA2 (breast cancer associated gene 2; identical to Rabring7, ZNF364 or RNF115) as a novel tetherin-interacting protein that enhances tetherin-dependent viral restriction. BCA2 was found to facilitate the internalization of HIV-1 particles captured by tetherin on the plasma membrane by associating with the cytoplasmic tail of tetherin and directing the degradation of viral particles in lysosomes. Significantly, the targeted depletion of BCA2 was found to reduce the intracellular accumulation of viral particles and to increase the persistence of nascent virions on the plasma membrane. Our current results thus reveal that BCA2 is a potential antiviral host factor through its collaboration with tetherin and is therefore a potential new therapeutic target for AIDS and its related disorders.

Results

Identification of BCA2 as a tetherin-interacting protein

The precise mechanism in which HIV-1 particles undergo internalization and/or degradation in cells following tetherin-mediated capture on the plasma membrane has not been well characterized. However, accumulating evidence now suggests that plasma membrane-tethered virions transit the small G protein Rab-dependent endocytotic pathway [6,15]. To delineate the molecular determinants that regulate this process, we attempted to identify the Rab family member or its effector proteins that functionally interact with tetherin. As our initial screening test, we performed immunoprecipitation and GST-pull down analyses to examine the interaction of approximately 60 Rab family proteins with either tetherin or HIV-1 Gag protein. These in vitro interaction assays revealed that a Rab7-interacting protein, BCA2, could interact with tetherin (data not shown). To further confirm this interaction, we performed GST-pull down analysis with recombinant GST-BCA2. 293T cells were transfected with either N-terminal Myc-epitope-tagged wild-type tetherin or its deletion mutant devoid of the cytoplasmic tail domain (tetherinΔ1–20). Cell lysates were then subjected to GST-pull down analysis with either GST alone or GST-BCA2. Consequently, GST-BCA2 was found to interact with full-length tetherin in cell lysates, but to interact less efficiently with tetherinΔ1–20 (Fig. 1A). This result was further confirmed by immunoprecipitation analysis using 293T cells transfected with either Myc-tetherin or Myc-tetherinΔ1–20 together with an N-terminal HA-tagged BCA2 construct (Fig. 1B).

BCA2 contains an N-terminal Rab7 binding domain and a C-terminal RING domain [26]. To investigate which of these is involved in the interaction with tetherin, we constructed BCA2 derivatives lacking these domains for use in immunoprecipitation analysis. Our results demonstrated that Myc-tetherin is efficiently coimmunoprecipitated with the full length BCA2, the N-terminal truncation mutant, BCA2ΔN (148–305 aa) or the RING domain deleted mutant, BCA2ΔRING (1–227 aa) (Fig. 1C). However, the C-terminal truncation mutant, BCA2ΔC (1–147 aa), showed no detectable interaction with Myc-tetherin (Fig. 1C). These results suggest that tetherin can interact with the middle portion of BCA2 (147–227 aa) located between the Rab-interacting domain and RING finger domain. We also confirmed an interaction between endogenous BCA2 and tetherin in HeLa cells (Fig. 1D), where these proteins were verified to be endogenously expressed (Fig. S1).

To further verify the association between BCA2 and tetherin in cells, we examined the intracellular localization of these two proteins using confocal microscopy. Immunofluorescent analysis revealed that N-terminal GFP-tagged tetherin and HA-BCA2 show a similar distribution in cells and form multiple cytoplasmic dots when they are expressed alone (Fig. 1E). When GFP-tetherin and HA-BCA2 are co-transfected however, these proteins show a significant co-localization predominantly in the cytoplasm, but also in part at the plasma membrane (Fig. 1E). These results together indicate that BCA2 is a tetherin-interacting protein that associates with the cytoplasmic tail of tetherin in cells.

BCA2 facilitates the restriction of HIV-1 particle production in cells expressing tetherin

We next examined the effects of BCA2 upon HIV-1 particle production in both endogenously tetherin-positive HeLa cells and in tetherin-negative HOS cells. Endogenous tetherin expression on the cell surface was confirmed by flow cytometric analysis (Fig. S1A). Cells were transfected with different amounts of HA-BCA2 together with either the HIV-1 proviral plasmid (pNL4-3) [27] or a Vpu-deleted version of this construct (pNL4-3ΔVpu) [14]. After 48 hours, cell supernatants were assayed for the Gag p24 antigen. Strikingly, the expression of BCA2 in tetherin-positive HeLa cells led to a strong restriction of HIV-1 particle production. Importantly, the restriction of Vpu-deleted HIV-1 was more prominent than that of the WT virus in HeLa cells (Fig. 2A). However, there was no significant suppressive effect of BCA2 on viral particle production in tetherin-negative HOS cells (Fig. 2A). This indicated that BCA2 reduces HIV-1 particle production in the presence of tetherin. Consistent with this observation, HOS cells exogenously expressing relatively low amounts of tetherin, but not the tetherinΔ1–20 mutant, showed BCA2-mediated restriction of HIV-1 particle production (Fig. 2B).

Since Vpu has been shown to antagonize the antiviral activity of tetherin [6,7], we next investigated whether Vpu could also counteract the antiviral effects of BCA2. As expected, Vpu-defective HIV-1 particle production was almost completely recovered by the expression of Vpu in HeLa cells (Fig. 2C). However, the co-expression of BCA2 significantly suppressed the recovery of virus particle production by Vpu (Fig. 2C). Conversely, the expression of a truncated Vpu mutant (Vpu1–50), the function of which is partly impaired [6], only partially counteracted HIV-1

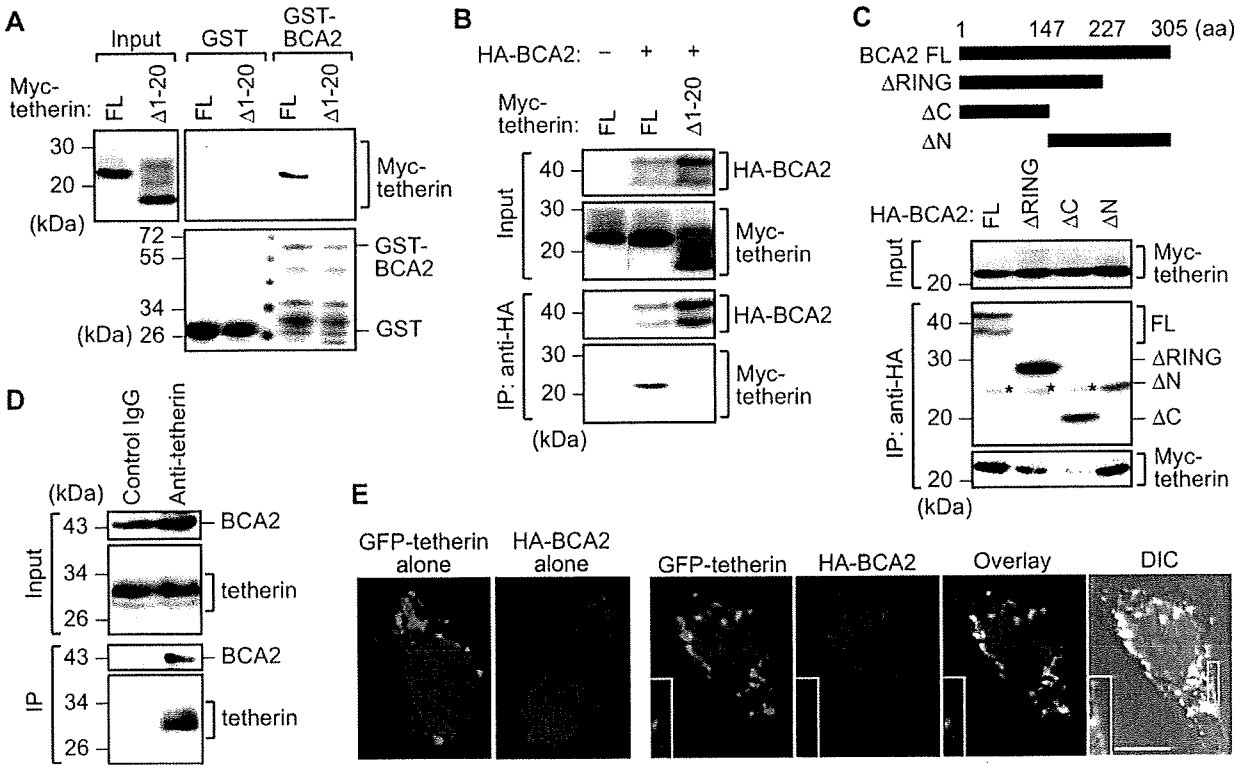

Figure 1. BCA2 is a tetherin-interacting protein. (A) GST pull-down analysis of 293T cells expressing either N-terminally Myc-tagged-tetherin (FL) or a mutant lacking the cytoplasmic tail domain (Δ1–20). Cell lysates were precipitated with either purified GST or GST-BCA2, followed by immunoblotting analysis with a Myc antibody to detect BCA2 binding (top panels). To control for the expression levels of GST, a Coomassie Brilliant Blue stained image is also shown (bottom panel). (B) Immunoprecipitation analysis of 293T cells expressing N-terminally HA-tagged-BCA2 together with either Myc-tetherin (FL) or its mutant (Δ1–20). Cell lysates were immunoprecipitated with HA antibodies, followed by immunoblotting analysis with either HA or Myc antibodies. (C) Immunoprecipitation analysis of 293T cells expressing Myc-tetherin together with HA-BCA2 (FL) or its deletion mutants (ΔRING, ΔC and ΔN). Asterisks indicate non-specific IgG bands. (D) Immunoprecipitation analysis of endogenous tetherin and BCA2. HeLa cell lysates were immunoprecipitated with either anti-tetherin monoclonal antibody or control mouse IgG followed by immunoblotting with the indicated antibodies. (E) Confocal microscopic analysis of HeLa cells expressing GFP-tagged tetherin and HA-BCA2 (scale bar, 10 μm). Cells were fixed, permeabilized and stained with HA antibodies (red) followed by confocal microscopy. The inset shows an expanded view of the area indicated by the white box in which an association of GFP-tetherin with HA-BCA2 at the plasma membrane is evident.
doi:10.1371/journal.ppat.1000700.g001

restriction by BCA2 (Fig. 2C). These results indicate that a functional Vpu antagonizes the restrictive activity of BCA2. Together with our finding that BCA2 can restrict HIV-1 particle production only in tetherin-expressing cells, these data indicate that the function of tetherin, which is antagonized by Vpu, is likely required for the BCA2-mediated restriction of HIV-1 particle production.

Previous studies have demonstrated that BCA2 has E3 ubiquitin ligase activity which is essential for the downregulation of EGFR expression [28]. We therefore examined whether this activity is necessary for the anti-viral effects of BCA2. We created a RING finger-defective mutant BCA2 (C228A/C231A) [29] and investigated its effect upon virus particle production. Although a tetherin-interacting motif defective BCA2 mutant (BCA2ΔC) failed to restrict viral particle production, both WT and C228A/C231A BCA2 were capable of doing so (Fig. 2D). Moreover, the effect of C228A/C231A BCA2 mutant was modest increase than that of WT BCA2 (Fig. 2D), probably due to the inhibition of both auto-ubiquitination and following degradation of this mutant as reported previously [28]. These results indicate that the ubiquitin ligase activity of BCA2 is dispensable for its function in the restriction of virus particle formation.

To next investigate the effects of BCA2 upon virus particle restriction in T cells, we created Jurkat cells stably expressing untagged BCA2 (Fig. 2E). FACS analysis with a tetherin antibody revealed that these cells indeed express tetherin on their cell surface (Fig. S1A). The cells were then infected with either HIV-1_{NL4-3} or HIV-$1_{NL4-3}\Delta_{Vpu}$ at a low multiplicity of infection (m.o.i. = 0.05). In agreement with a previous report [11], we found that Vpu-deleted virus replicated slightly less efficiently than WT-virus (Fig. 2E). Our results showed that BCA2 expression reduces HIV-1 particle production in both WT- and ΔVpu-virus infected cells, although this effect was more prominent in cells infected with ΔVpu-virus (about 4-fold) than with WT-virus (about 2-fold) (Fig. 2E). Interestingly, immunoblotting analysis revealed that the expression levels of endogenous BCA2 in HeLa and Jurkat cells were relatively lower than in HOS cells (Fig. S1B), implying that exogenous BCA2 expression would tend to impact virus particle restriction in these cells in the presence of functional tetherin.

To delineate the molecular mechanism by which BCA2 suppresses virus production, we performed immunoblotting analysis with a p24 antibody. Interestingly, the expression of BCA2 in HeLa cells significantly reduced the Gag protein

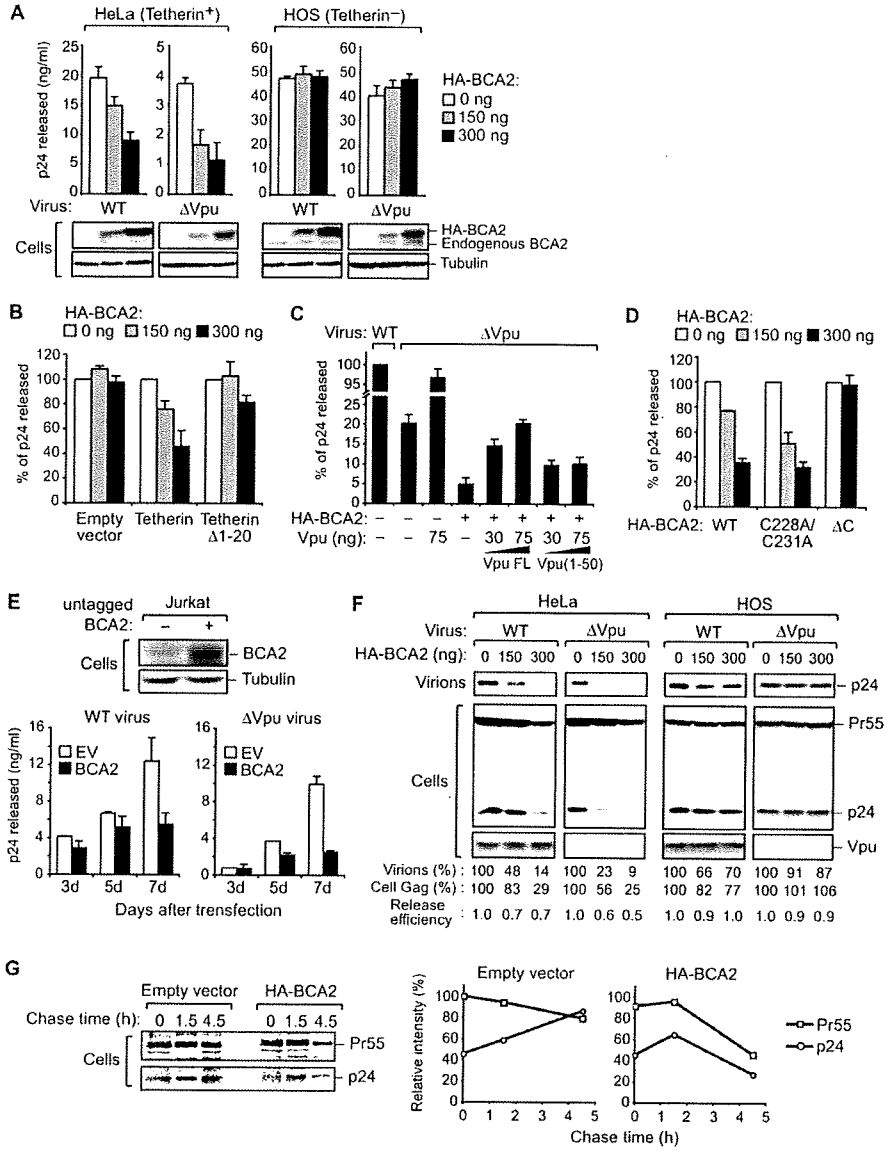

Figure 2. BCA2 inhibits HIV-1 particle production in cells expressing tetherin. (A) Single-round virus release analysis was performed using the indicated cell types transfected with either 300 ng of pNL4–3 or pNL4–3ΔVpu along with the indicated amounts of pCMV-HA-BCA2. At 48 hours following transfection, cell supernatants were analyzed by p24 ELISA. Immunoblotting with a BCA2 antibody for both endogenous and HA-tagged BCA2 expression is shown in the bottom panels. (B) Tetherin-dependent effects of BCA2 on HIV-1 particle production. HOS cells were transiently transfected with 100 ng of pCMV-Myc-tetherin or its deletion mutant (Δ1–20, lacking the cytoplasmic tail) together with 300 ng of pNL4–3 and indicated amounts of pCMV-HA-BCA2, followed by p24 ELISA. (C) Vpu antagonizes the effects of BCA2 upon HIV-1 particle production. HeLa cells were transiently transfected with either the indicated amounts of Vpu or its deletion mutant (1–50, lacking a portion of the cytoplasmic domain) and 300 ng of pNL4–3ΔVpu was co-transfected with or without 300 ng of pCMV-HA-BCA2. After 48 hours, cell supernatants were analyzed by p24 ELISA. (D) Single-round virus release analysis was performed using HeLa cell transfected with 300 ng of pNL4–3 along with either pCMV-HA-BCA2 (WT), its RING finger-defective mutant (C228A/C231A) or tetherin-interacting motif defective BCA2 mutant (ΔC). At 48 hours following transfection, viral supernatants were analyzed by p24 ELISA. (E) Jurkat cells were transfected with either empty vector (EV) or pIRESpuro-BCA2 by electroporation and selected with puromycin for 24 hours. The stable expression of BCA2 on Jurkat cells was confirmed by BCA2 immunoblotting (top panel). Cells were then infected with either HIV-1_{NL4-3} or HIV-$1_{NL4-3}\Delta_{Vpu}$ at a low multiplicity. Cell supernatants were harvested at the indicated time-points and subjected to p24 ELISA (bottom panel). (F) BCA2 reduces the level of cell-associated Gag protein. Immunoblotting analysis of the cell lysates described in (A) was performed. The numerical values below the blots indicate the Gag signal intensities determined by densitometry. The virus release efficiency was calculated as "Sup Gag per Total Gag (Cell Gag plus Sup Gag)". (G) Pulse-chase analysis of HeLa cells transfected with pNL4–3ΔVpu together with either control vector or pCMV-HA-BCA2. Two days after transfection, the radiolabeled cells were harvested at the indicated times, and cell lysates were immunoprecipitated with anti-p24 antibody, and then analyzed by SDS-PAGE and autoradiography (left panel). The relative intensity of Gag bands was determined by densitometry (right panel).
doi:10.1371/journal.ppat.1000700.g002

levels, particularly cell-associated p24, but had no effect upon the expression of Vpu (Fig. 2F). Our results also indicate that BCA2 expression has modest effects on viral release efficiency as compared with its drastic effects on the cell-associated p24 protein levels (Fig. 2F). Of note, the BCA2-induced depletion of cell-associated p24 in the absence of Vpu was more prominent than in the presence of Vpu (Fig. 2F). These data together suggest that BCA2 may enhance the degradation of nascent HIV-1 virions captured by tetherin on the plasma membrane.

To rule out the possibility that BCA2 affects the expression of HIV-1 proteins, we next performed pulse-chase analysis with pNL4-3ΔVpu-transfected HeLa cells. Our results demonstrated that BCA2 expression induces the rapid degradation of the HIV-1 Gag protein (Fig. 2G). Consistent with our immunoblotting data (Fig. 2F), the degradation of p24 was shown to be more prominent than that of Pr55 (Fig. 2G). Furthermore, our RT-PCR analysis revealed that BCA2 expression does not significantly affect the mRNA levels of HIV-1 Gag (Fig. S2). These results together indicate that BCA2 facilitates the intracellular degradation of virus particles rather than the suppression of HIV-1 protein expression.

BCA2 promotes the accumulation of HIV-1 virions in intracellular compartments

As described above, the expression of BCA2 significantly reduces the level of cell-associated p24 protein, raising the possibility that it facilitates the intracellular degradation of unreleased virions. To test this possibility, we performed transmission electron microscopy (TEM) analysis of HeLa cells transduced with proviral plasmid together with either HA-BCA2 or a control vector. In control cells, nascent assembled virions were observed on the plasma membrane and relatively little accumulation of virions was observed in intracellular compartments (Fig. 3A). In BCA2-expressing cells, however, substantial numbers of mature virions could be observed in the intracellular vesicles, and a significant reduction of mature viral particles on the plasma membrane was found (Fig. 3B). This suggests that BCA2 facilitates the internalization of mature viral particles into intracellular vesicles for degradation.

BCA2 enhances the targeting of HIV-1 virions for lysosomal degradation

Consistent with our TEM results, immunofluorescent and confocal microscopic analysis further revealed that BCA2 expression promotes the accumulation of p24 in $CD63^+$ intracellular compartments when compared with the vector control (Figs. 4A, B). Various proteins that are sorted into $CD63^+$ intracellular compartments are destined for lysosomal degradation [30,31]. To address whether virion degradation is mediated by this pathway following internalization, we co-transfected HeLa cells with the HIV-1 proviral plasmid together with either empty vector or HA-BCA2, and then treated the cells with lysosome inhibitors (leupeptin and NH_4Cl). Strikingly, treatment with lysosome inhibitors significantly blocked the decrease in intracellular Gag in BCA2-expressing cells (Fig. 4C). Importantly also, parallel ELISA analysis of the supernatants from these transduced cells revealed that lysosome inhibitors had no effect upon viral release (Fig. 4D). These results suggest that BCA2 promotes the lysosomal degradation of HIV-1 virions following their retention on the plasma membrane and subsequent internalization into $CD63^+$ endosomes.

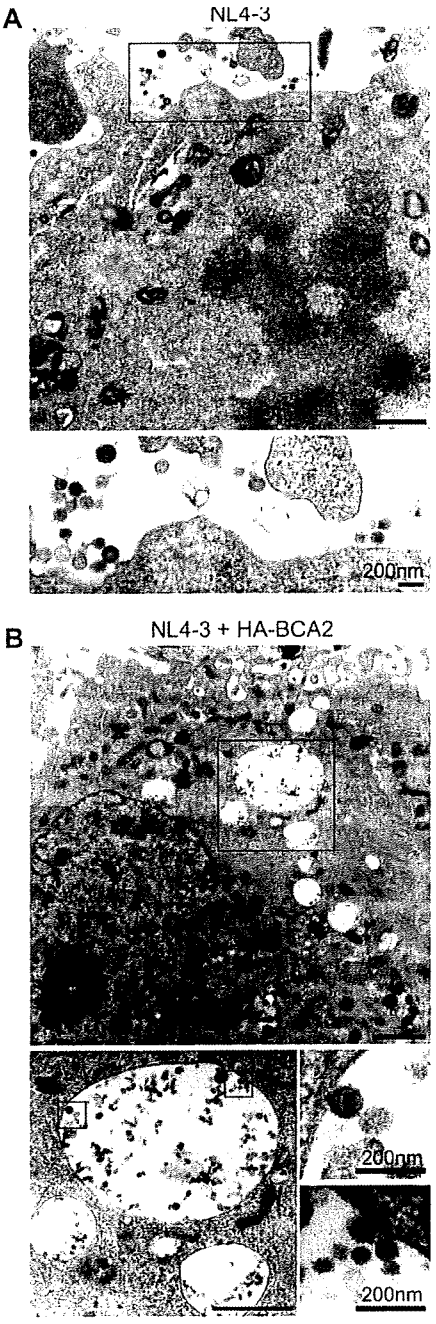

Figure 3. BCA2 promotes the accumulation of HIV-1 virions in intracellular compartments. Electron microscopic analysis of HeLa cells transfected with pNL4–3 and either control vector (A) or pCMV-HA-BCA2 (B), at a molar ratio of 1:3. (Scale bars, 1 μm except where indicated).
doi:10.1371/journal.ppat.1000700.g003

The targeted depletion of BCA2 reduces the intracellular accumulation of HIV-1 particles

To further delineate the role of endogenous BCA2 in HIV-1 particle release, we next performed experiments in which HeLa cells were transduced with either control or two different BCA2-specific siRNAs (BCA2-I, II) and then transfected with pNL4-3 or

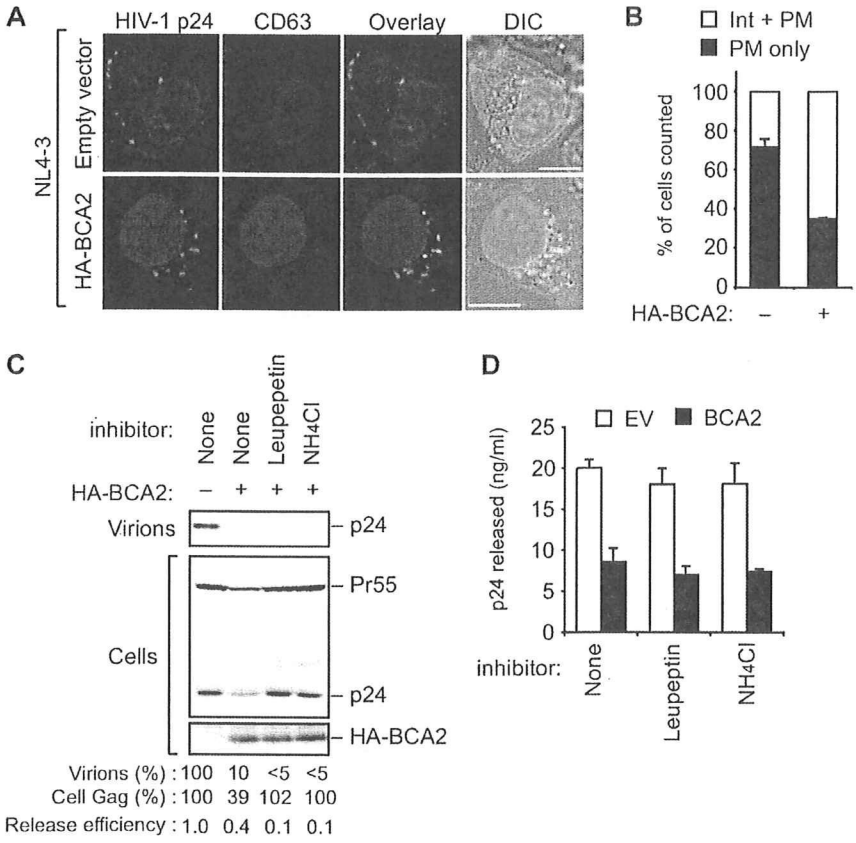

Figure 4. BCA2 enhances HIV-1 virion trafficking to lysosomes. (A) Confocal microscopic analysis of HeLa cells expressing pNL4–3 and either empty vector (top row) or pCMV-HA-BCA2 (bottom row), at a molar ratio of 1:3 (scale bar, 10 μm). Note that these transfected cells also expressed Vpu. Cells were stained with anti-p24 (green) and anti-CD63 (red) antibodies and analyzed by confocal microscopy. (B) In the cultures described in (A), over 100 cells were analyzed for the subcellular localization of p24, which was either strongly evident at the plasma membrane (PM only), or intracellular accumulations as well as at the plasma membrane (Int + PM). The data are given as a percentage of the total cells. (C, D) HeLa cells transfected with 300 ng of pNL4–3 and either empty vector or pCMV-HA-BCA2, at a molar ratio of 1:3, were treated with or without lysosomal inhibitors. Inhibitors were added to the medium 18 hours before harvesting. Cell lysates and supernatants were then analyzed by immunoblotting (C) and p24 ELISA (D). The final concentrations of leupeptin and NH_4Cl were 5 μg/ml and 2 mM, respectively. The Gag signal intensities and the virus release efficiency are shown below the blots, as in Fig. 2F.
doi:10.1371/journal.ppat.1000700.g004

pNL4-3ΔVpu. Immunoblotting analysis with a BCA2 antibody demonstrated that both of the siRNAs targeting BCA2 could significantly reduce its endogenous expression (Fig. 5A). Measurement of the p24 antigen levels in the cell supernatant further revealed that viral particle production was only slightly increased in both pNL4-3 and pNL4-3ΔVpu transfected cells, although the effect was more significant in pNL4-3ΔVpu transfected cells (approximately 2-fold) (Fig. 5A).

Immunofluorescent analysis by confocal microscopy additionally revealed that although the localization of Gag proteins was observed predominantly in $CD63^+$ intracellular structures in control-siRNA treated cells, this profile was dramatically shifted to the plasma membrane in BCA2-siRNA treated cells (Figs. 5B, C). This indicated that the silencing of BCA2 blocks the relocation of virions into the intracellular compartments and increases the persistence of virions captured by tetherin on the cell surface.

To further investigate this possibility, siRNA-transduced cells were subsequently treated with the protease subtilisin, which liberates cell surface-captured virions by abolishing virion-tetherin interactions [15]. In the case of WT-virus, subtilisin stripping had only slight effects upon virion release (Fig. 5D), in agreement with a previous report [15]. However, in the case of Vpu-defective virus, viral release from BCA2-deplation cells was significantly recovered by subtilisin stripping, reaching the level of WT-virus infected cells (Fig. 5D). These data suggest that BCA2 depletion inhibits the intracellular accumulation of Gag proteins and, consequently, increases the fraction of virions retained at the cell surface by tetherin.

Overall, the results of our current study indicate that BCA2 facilitates the internalization of HIV-1 virions that have not been released, thereby enhancing their degradation. This internalization and degradation of cell surface-retained virions may represent rate limiting steps in the tetherin-mediated restriction of viral release that are accelerated by BCA2.

Discussion

In our current study, we identify BCA2 as a functional tetherin-interacting protein. Although BCA2 is widely expressed in various cell lines [26,32], its antiviral effects have been observed only in cells expressing tetherin, suggesting that BCA2 cooperates with tetherin to achieve efficient restriction of viral particle production. BCA2

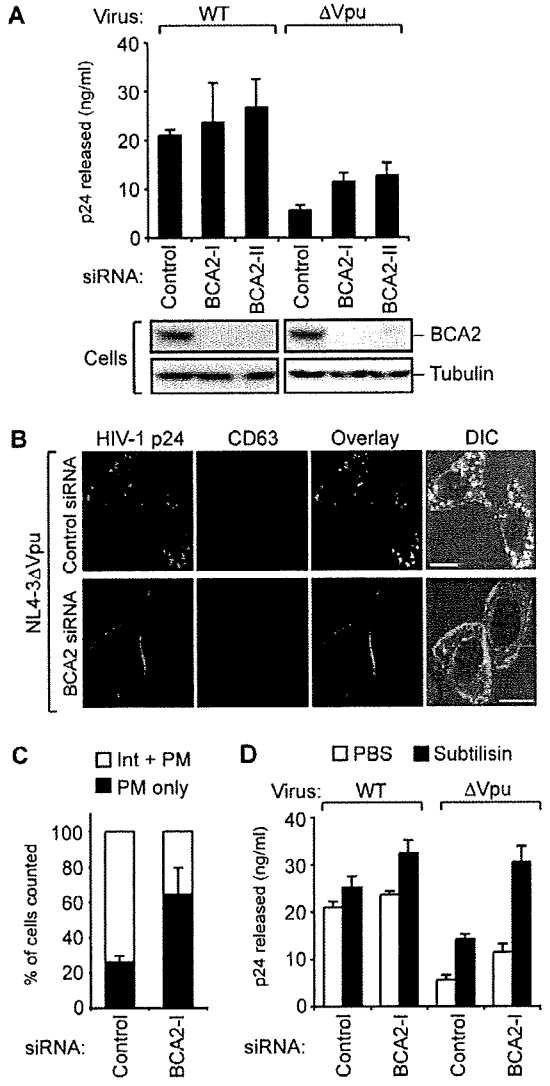

Figure 5. The targeted depletion of BCA2 blocks the intracellular accumulation of viral particles. (A) Single-round virus release analysis of HeLa cells treated with control siRNA or two different BCA2-targeted siRNA vectors for 24 hours, prior to transfection with pNL4-3 or pNL4-3ΔVpu. At 48 hours following transfection, cell supernatants were analyzed by p24 ELISA. Immunoblotting analysis with a BCA2 antibody to detect endogenous BCA2 expression is shown in the bottom panel. (B) Confocal microscopic analysis of HeLa cells treated with control siRNA (upper panels) or BCA2-targeted siRNA (lower panels), prior to transfection with pNL4-3ΔVpu (scale bar, 10 μm). After 48 hours following transfection, cells were fixed and immunostained with anti-p24 (green) and anti-CD63 (red) antibodies followed by confocal microscopy. (C) In the cultures described in (B), over 100 cells were analyzed for the subcellular localization of p24, as described in Fig. 4B. (D) HeLa cells were treated with control siRNA or BCA2-targeted siRNA for 24 hours, prior to transfection with pNL4-3 or pNL4-3ΔVpu as in (A). At 48 hours following transfection, cell supernatants were harvested (first supernatants) and cells were treated with either PBS or buffer containing the protease subtilisin (1 mg/ml) for 15 min, prior to re-harvesting of the cell supernatants (second supernatants). Both the first and second supernatants were then mixed and analyzed by p24 ELISA.

doi:10.1371/journal.ppat.1000700.g005

was found in our current analyses to play a crucial role in the internalization and degradation of nascent HIV-1 virions, following their tethering to the host cell plasma membrane. These internalization and degradation steps may be rate limiting during restriction by tetherin because the targeted depletion of BCA2 can shift the distribution of Gag to the plasma membrane and can partly overcome the release inhibition of Vpu-minus virions in HeLa cells.

Importantly in this regard, BCA2 directs HIV-1 particles to $CD63^+$ endosomes or lysosomes for degradation. The molecular mechanisms by which this is achieved have not yet been fully characterized. However, previous studies have demonstrated that BCA2 directly binds a small G protein, Rab7, and thereby plays crucial roles in vesicle trafficking to the late endosomes or lysosomes, in addition to lysosome biogenesis [26,33]. Indeed, the aberrant expression of BCA2 not only affects epidermal growth factor receptor (EFGR) degradation, but also induces the perinuclear aggregation of lysosomes and increased acidity within lysosomes [26,28]. Given our current data, these results indicate that BCA2 coordinates the trafficking of intracellular vesicles containing internalized viral particles to the lysosomes in conjunction with Rab7, resulting in the effective degradation of these virions. Consistently, in tetherin-positive HeLa cells, Gag protein has been shown to co-localize with the GTP-bound active form of Rab7 in the absence of Vpu (our unpublished observation). Furthermore, a dominant negative mutant of Rab5 can inhibit the internalization of nascent HIV-1 particles [15]. These findings raise the possibility that plasma membrane-tethered virions may go through a Rab5- and/or Rab7-dependent endocytotic pathway from the cell surface to the endosomes or lysosomes and eventual degradation. Notably, our immunoprecipitation data indicate that BCA2 interacts with tetherin at a region distinct from the Rab7 binding site. Consistently, an N-terminal truncation mutant of BCA2 can still interact with tetherin. These results suggest that BCA2 may simultaneously interact with Rab7 and tetherin at distinct regions and might therefore act as a physical scaffolding protein between these two proteins. During endocytosis, tetherin-BCA2 complexes might therefore recruit Rab7 to vesicles containing virions.

Although the function of BCA2 during HIV-1 restriction is likely to be dependent on tetherin, the antiviral effects of BCA2 were found to be still active against Vpu-positive viruses. However, the overexpression of Vpu can abrogate the antiviral effects of BCA2, indicating a potentially stoichiometric relationship between BCA2 and Vpu during BCA2-mediated viral restriction. Importantly, our current results suggest that BCA2 is not involved in regulating the expression of Vpu. However, it is possible that BCA2 antagonizes the function of Vpu in counteracting tetherin, although further analysis is needed to address this question.

Our current results additionally demonstrate that the effects of BCA2 depletion on particle production are about two-fold, which is a relatively modest impact compared with the 5-to-10-fold effects of Vpu in tetherin-positive cells. This indicates that the inhibition of BCA2 cannot fully restore Vpu-defective HIV-1 particle production to the level of the WT-virus. Apparently, capture of virions on the plasma membrane by tetherin provides restriction even when BCA2-depletion suppresses the internalization and degradation of nascent virions. These effected were further revealed by our subtilisin stripping assay; BCA2-depletion plus subtilisin treatment recovered ΔVpu-virus particle production to the level of the WT-virus. These results indicate that BCA2 very likely functions downstream of virus tethering on the plasma membrane (i.e. post-tethering stages).

In summary, the results of our current study demonstrate that BCA2 is a potential anti-HIV-1 host factor that partners with

tetherin to facilitate the internalization and degradation of nascent viral particles. Our present findings thus shed new light on the molecular machinery underlying the tetherin-dependent HIV-1 restriction pathway. BCA2 and other molecules of this pathway may thus be potential new therapeutic targets for AIDS and its related disorders.

Materials and Methods

Cells and transfections

HeLa, HOS and 293T cells were cultured in DMEM supplemented with 10% fetal bovine serum (FBS). Jurkat cells were maintained in RPMI-1640 containing 10% FBS. Plasmid transfections into adherent or suspended cells were performed using Lipofectamine 2000 (Invitrogen, Carlsbad, CA) or Amaxa nucleofector (Program S-18; Amaxa biosystems, Cologne, Germany), respectively, according to the manufacturer's instructions.

Plasmids and viruses

Human BCA2 and tetherin/CD317 coding sequences were amplified from HeLa total RNA by RT-PCR using the following pairs of oligonucleotides containing restriction enzyme BamHI sites (underlined) or a stop codon (boldface): 5′-GGATCCGGATGGCGGAGGCTTCGGCGGC-3′ (BCA2 forward primer, sense) and 5′-**TCA**GAAAGTCCATCGGTCATG-3′ (BCA2 reverse primer, antisense); 5′-GGATCCGGATGGCATCTACTTCGTATGA-3′ (tetherin forward primer, sense) and 5′-**TCA**CTGCAGCAGAGCGCTGAGGC-3′ (tetherin reverse primer, antisense). The purified PCR products were inserted into the pCR4Blunt-TOPO vector (Invitrogen), and cDNA inserts were then subcloned into pCMV-HA, pCMV-Myc, pEGFP-C1, pIRESpuro (Clontech, Palo Alto, CA) or pGEX-KG (Amersham Bioscience, Sunnyvale, CA) vectors. A human codon-optimized HIV-1 Vpu expression vector (pcDNA-Vphu) [34] and Vpu-deleted HIV-1 molecular clone (pNL4-3/Udel, herein called pNL4-3ΔVpu) [14] were kindly provided by Dr. K. Strebel (National Institutes of Health, Bethesda, MD). The ΔRING (1-227 aa), ΔN (148-305 aa), ΔC (1-147 aa), and C228A/C231A derivatives of BCA2, the tetherin mutant Δ1-20 (21-180 aa) and the truncated Vpu mutant (1-50 aa) were constructed using standard molecular cloning procedures. The WT-virus or ΔVpu-virus stocks were produced by transient transfection of 293T cells with the pNL4-3 or pNL4-3ΔVpu proviral plasmids, respectively. Culture supernatants containing virus were collected 48 hours after transfection, filtered through a 0.45 μm Millex-HV filter (Millipore, Billerica, MA) and immediately stored at −80°C until use.

Antibodies

An anti-BCA2 polyclonal antibody was produced by UNITECH (Chiba, Japan). An anti-p24 monoclonal antibody has been described previously [35]. The rabbit anti-Vpu and mouse anti-HM1.24 (tetherin) antibodies were kindly donated by Dr. K. Strebel (National Institutes of Health, Bethesda, MD) [36] and Chugai Pharmaceutical Co. (Kanagawa, Japan) [37], respectively. Other antibodies used in this study were as follows: mouse anti-HA (Roche, Basel, Switzerland), mouse anti-Myc (Roche), mouse anti-α-tubulin (Sigma, St. Louis, MO), rabbit anti-CD63 (Santa Cruz Biotechnology, Santa Cruz, CA) and Alexafluor-conjugated anti-IgG (Invitrogen).

In vitro binding assays

For GST pull-down assays, GST-tagged BCA2 was expressed in *Escherichia coli* BL21 (DE3) cells and purified using standard protocols. Myc-tetherin-expressing 293T cell lysates were incubated with glutathione-beads that had been coupled with GST-BCA2 proteins. The beads were then washed, and bound proteins were visualized by Coomassie Brilliant Blue R-250 staining and analyzed by immunoblotting. For immunoprecipitation analysis, 293T cells expressing Myc-tetherin and HA-BCA2 were lysed and incubated with an anti-HA affinity gel (Sigma). Alternatively, to detect endogenous tetherin-BCA2 complexes, HeLa cell lysates were co-incubated with protein A/G-mixed Sepharose (GE Healthcare, UK) and either anti-tetherin antibody or control mouse IgG. Bound proteins were analyzed by SDS-PAGE and immunoblotting.

Single-round viral release and multi-cycle replication assays

Cells in 12-well plates were co-transfected with pNL4-3 or pNL4-3ΔVpu (300 ng) and either pCMV-HA-BCA2 or empty vector (0-300 ng), in the presence or absence of vectors encoding Vpu (30 or 75 ng) or Myc-tetherin (100 ng). Two days after transfection, virus-containing supernatants were harvested and filtrated to remove debris, and p24 antigens were measured by Lumipulse (Fujirebio, Tokyo, Japan). For immunoblotting assays, the virus-containing supernatants (400 μl) was layered onto 600 μl of 20% sucrose in PBS and centrifuged at 20,000 *g* for 2 hours at 4°C. The cell lysates were prepared using RIPA buffer by incubation at 4°C for 10 minutes and centrifugation at 16,000 *g* for 30 minutes. In experiments using lysosomal inhibitors, each drug was added 18 hours before harvesting. Immunoblotting band intensities were quantitated with ImageJ software.

For multi-cycle replication assays, Jurkat cells (1×10^6) were transfected with either empty vector or pIRESpuro-BCA2 (3 μg). After the selection of transfectants with puromycin for 24 hours, cell aliquots were then infected with either HIV-1_{NL4-3} or HIV-$1_{NL4-3}\Delta_{Vpu}$ at an m.o.i of 0.05. Viral supernatants were collected periodically, and p24 levels were measured as described above.

Microscopy

One day prior to transfection, HeLa cells were seeded onto glass-bottom dishes coated with poly-L-lysine (Matsunami, Osaka, Japan). At 48 hours after transfection, the cells were fixed with 4% paraformaldehyde and permeabilized with 1% Triton X-100. Cells were than stained with primary antibodies and Alexa-conjugated secondary antibodies. Confocal microscopic imaging was performed using a Zeiss LSM510 instrument equipped with a 63× oil-immersion objective. For electron microscopy, transfected HeLa cells were fixed with 2.5% glutaraldehyde and subjected to transmission electron microscopy, as described previously [38].

Pulse-chase radiolabeling

Cells in 6-well plates were co-transfected with pNL4-3ΔVpu (1 μg) and either pCMV-HA-BCA2 or empty vector (3 μg). Two days after transfection, the cells were washed and starved in Met-/Cys-depletion medium (Invitrogen) for 30 min and pulse-labeled for 15 min with 0.25 mCi/ml of [^{35}S]Met-Cys medium, and chased in unlabeled medium for 4.5 hours. Cells were harvested periodically, and cell lysates were immunoprecipitated with anti-p24 antibody, and then analyzed by SDS-PAGE and autoradiography.

siRNA knockdown and subtilisin stripping assays

BCA2-targeted siRNAs were obtained from Invitrogen as Stealth Select RNAi constructs (Oligo ID #HSS120532 and #HSS120534). A Stealth RNAi Luciferase reporter control

(Invitrogen) was used as the negative control siRNA. Cells in 12-well plates were transfected with these siRNAs at a final concentration of 50 μM using Lipofectamine RNAiMAX (Invitrogen). The following day, the cells were re-transfected with 300 ng of either pNL4-3 or pNL4 3ΔVpu, and two days later were harvested and analyzed by immunoblotting or confocal microscopy.

For protease subtilisin stripping assays, viral supernatants (1.2 ml) from siRNA/DNA-transfected HeLa cells were harvested as a "first supernatant". After harvesting, the cells were washed once with pre-warmed PBS and then incubated with 300 μl of either PBS or Tris/HCl (pH 8.0) buffer containing 1 mg/ml subtilisin (Sigma) for 15 min at 37°C. To stop the reaction, 900 μl of DMEM containing 5 mM PMSF were added to the cells, and supernatants (total 1.2 ml) were again harvested as a "second supernatant". Both the first and second supernatants were then mixed and the p24 levels were measured as described above.

Accession numbers

The GenBank accession numbers for human BCA2 (Rabring7/ZNF364/RNF115) and human tetherin (CD317/BST-2/HM1.24) are BC054049 and D28137, respectively.

Supporting Information

Figure S1 Endogenous expression of tetherin and BCA2 in the cells used in this study. (A) Flow cytometric analysis of cell surface tetherin expression in HeLa, HOS and Jurkat cells. Cells were washed with ice-cold PBS containing 1% BSA, and were blocked for 10 min with 10% normal goat serum. The cells were then stained with an anti-tetherin monoclonal antibody (0.1 μg/ml) and a PE-conjugated secondary antibody (Beckman Coulter, Fullerton, CA). All samples were analyzed with a FACS Caliber (BD Biosciences, San Jose, CA). (B) Immunoblotting analysis of the indicated cell lysates. Blots were probed with either anti-BCA2 or anti-α-tubulin antibodies.
Found at: doi:10.1371/journal.ppat.1000700.s001 (0.20 MB PDF)

Figure S2 BCA2 has no detectable effects on the Gag RNA levels. RT-PCR analysis of total RNA extracted from HeLa cells transfected with pNL4-3 and either control vector or pCMV-HA-BCA2 at a molar ratio of 1:1. The PCR primers were as follows: 5′-CCCTATAGTGCAGAACCTCCA-3′ (p24CA RT-forward) and 5′-CATTATGGTAGCTGGATTTGTTAC-3′ (p24CA RT-reverse); 5′-GATCCGGTACTAGAGGAACTGAAAAAC-3′ (Exogenous BCA2 RT-forward) and 5′-TCACTGCAGCAGAGCGCTGAGGC-3′ (Exogenous BCA2 RT-reverse); 5′-ACGGATGGACTTTCTGAAGC-3′ (Endogenous BCA2 RT-forward) and 5′-AAGGCAACATGACAGACAGC-3′ (Endogenous BCA2 RT-reverse). The G3PDH RT-primers used have been described previously [35]. To clarify the differences between exogenous and endogenous BCA2, the exogenous BCA2 RT-forward primer contains a vector-derived sequence. Numerical values below the blots indicate the Gag signal intensities normalized to the G3PDH values determined by densitometry.
Found at: doi:10.1371/journal.ppat.1000700.s002 (0.08 MB PDF)

Acknowledgments

We thank Klaus Strebel and Chugai Pharmaceutical Co. for reagents, and Mayuko Nishi and Michiyo Kataoka for technical support. We also thank Andres Finzi for helpful suggestions.

Author Contributions

Analyzed the data: TM KO JG. Contributed reagents/materials/analysis tools: TM SY MF. Performed the research, collected and analyzed the data, and wrote the manuscript: KM. Designed and supervised research, collected and analyzed the data: AR. Designed the research, supervised, and commented on the manuscript: NY.

References

1. Goff SP (2007) Host factors exploited by retroviruses. Nat Rev Microbiol 5: 253-263.
2. Huthoff H, Towers GJ (2008) Restriction of retroviral replication by APOBEC3G/F and TRIM5alpha. Trends Microbiol 16: 612-619.
3. Freed EO (2004) HIV-1 and the host cell: an intimate association. Trends Microbiol 12: 170-177.
4. Malim MH, Emerman M (2008) HIV-1 accessory proteins-ensuring viral survival in a hostile environment. Cell Host Microbe 3: 388-398.
5. Neil SJ, Sandrin V, Sundquist WI, Bieniasz PD (2007) An interferon-alpha-induced tethering mechanism inhibits HIV-1 and Ebola virus particle release but is counteracted by the HIV-1 Vpu protein. Cell Host Microbe 2: 193-203.
6. Neil SJ, Zang T, Bieniasz PD (2008) Tetherin inhibits retrovirus release and is antagonized by HIV-1 Vpu. Nature 451: 425-430.
7. Van Damme N, Goff D, Katsura C, Jorgenson RL, Mitchell R, et al. (2008) The interferon-induced protein BST-2 restricts HIV-1 release and is downregulated from the cell surface by the viral Vpu protein. Cell Host Microbe 3: 245-252.
8. Jouvenet N, Neil SJ, Zhadina M, Zang T, Kratovac Z, et al. (2009) Broad-spectrum inhibition of retroviral and filoviral particle release by tetherin. J Virol 83: 1837-1844.
9. Sakuma T, Noda T, Urata S, Kawaoka Y, Yasuda J (2009) Inhibition of Lassa and Marburg virus production by tetherin. J Virol 83: 2382-2385.
10. Kaletsky RL, Francica JR, Agrawal-Gamse C, Bates P (2009) Tetherin-mediated restriction of filovirus budding is antagonized by the Ebola glycoprotein. Proc Natl Acad Sci U S A 106: 2886-2891.
11. Strebel K, Klimkait T, Martin MA (1988) A novel gene of HIV-1, vpu, and its 16-kilodalton product. Science 241: 1221-1223.
12. Cohen EA, Terwilliger EF, Sodroski JG, Haseltine WA (1988) Identification of a protein encoded by the vpu gene of HIV-1. Nature 334: 532-534.
13. Huet T, Cheynier R, Meyerhans A, Roelants G, Wain-Hobson S (1990) Genetic organization of a chimpanzee lentivirus related to HIV-1. Nature 345: 356-359.
14. Klimkait T, Strebel K, Hoggan MD, Martin MA, Orenstein JM (1990) The human immunodeficiency virus type 1-specific protein vpu is required for efficient virus maturation and release. J Virol 64: 621-629.
15. Neil SJ, Eastman SW, Jouvenet N, Bieniasz PD (2006) HIV-1 Vpu promotes release and prevents endocytosis of nascent retrovirus particles from the plasma membrane. PLoS Pathog 2: e39. doi: 10.1371/journal.ppat.0020039.
16. Willey RL, Maldarelli F, Martin MA, Strebel K (1992) Human immunodeficiency virus type 1 Vpu protein induces rapid degradation of CD4. J Virol 66: 7193-7200.
17. Willey RL, Maldarelli F, Martin MA, Strebel K (1992) Human immunodeficiency virus type 1 Vpu protein regulates the formation of intracellular gp160-CD4 complexes. J Virol 66: 226-234.
18. Chen MY, Maldarelli F, Karczewski MK, Willey RL, Strebel K (1993) Human immunodeficiency virus type 1 Vpu protein induces degradation of CD4 in vitro: the cytoplasmic domain of CD4 contributes to Vpu sensitivity. J Virol 67: 3877-3884.
19. Miyagi E, Andrew AJ, Kao S, Strebel K (2009) Vpu enhances HIV-1 virus release in the absence of Bst-2 cell surface down-modulation and intracellular depletion. Proc Natl Acad Sci U S A 106: 2868-2873.
20. Gottlinger HG, Dorfman T, Cohen EA, Haseltine WA (1993) Vpu protein of human immunodeficiency virus type 1 enhances the release of capsids produced by gag gene constructs of widely divergent retroviruses. Proc Natl Acad Sci U S A 90: 7381-7385.
21. Strebel K, Klimkait T, Maldarelli F, Martin MA (1989) Molecular and biochemical analyses of human immunodeficiency virus type 1 vpu protein. J Virol 63: 3784-3791.
22. Terwilliger EF, Cohen EA, Lu YC, Sodroski JG, Haseltine WA (1989) Functional role of human immunodeficiency virus type 1 vpu. Proc Natl Acad Sci U S A 86: 5163-5167.
23. Harila K, Prior I, Sjoberg M, Salminen A, Hinkula J, et al. (2006) Vpu and Tsg101 regulate intracellular targeting of the human immunodeficiency virus type 1 core protein precursor Pr55gag. J Virol 80: 3765-3772.
24. Harila K, Salminen A, Prior I, Hinkula J, Suomalainen M (2007) The Vpu-regulated endocytosis of HIV-1 Gag is clathrin-independent. Virology 369: 299-308.
25. Van Damme N, Guatelli J (2008) HIV-1 Vpu inhibits accumulation of the envelope glycoprotein within clathrin-coated, Gag-containing endosomes. Cell Microbiol 10: 1040-1057.
26. Mizuno K, Kitamura A, Sasaki T (2003) Rabring7, a novel Rab7 target protein with a RING finger motif. Mol Biol Cell 14: 3741-3752.
27. Adachi A, Gendelman HE, Koenig S, Folks T, Willey R, et al. (1986) Production of acquired immunodeficiency syndrome-associated retrovirus in human and

nonhuman cells transfected with an infectious molecular clone. J Virol 59: 284–291.
28. Sakane A, Hatakeyama S, Sasaki T (2007) Involvement of Rabring7 in EGF receptor degradation as an E3 ligase. Biochem Biophys Res Commun 357: 1058–1064.
29. Amemiya Y, Azmi P, Seth A (2008) Autoubiquitination of BCA2 RING E3 ligase regulates its own stability and affects cell migration. Mol Cancer Res 6: 1385–1396.
30. Luzio JP, Rous BA, Bright NA, Pryor PR, Mullock BM, et al. (2000) Lysosome-endosome fusion and lysosome biogenesis. J Cell Sci 113: 1515–1524.
31. Piper RC, Luzio JP (2001) Late endosomes: sorting and partitioning in multivesicular bodies. Traffic 2: 612–621.
32. Burger AM, Gao Y, Amemiya Y, Kahn HJ, Kitching R, et al. (2005) A novel RING-type ubiquitin ligase breast cancer-associated gene 2 correlates with outcome in invasive breast cancer. Cancer Res 65: 10401–10412.
33. Burger A, Amemiya Y, Kitching R, Seth AK (2006) Novel RING E3 ubiquitin ligases in breast cancer. Neoplasia 8: 689–695.
34. Nguyen KL, llano M, Akari H, Miyagi E, Poeschla EM, et al. (2004) Codon optimization of the HIV-1 vpu and vif genes stabilizes their mRNA and allows for highly efficient Rev-independent expression. Virology 319: 163–175.
35. Ohba K, Ryo A, Dewan MZ, Nishi M, Naito T, et al. (2009) Follicular dendritic cells activate HIV-1 replication in monocytes/macrophages through a juxtacrine mechanism mediated by P-selectin glycoprotein ligand 1. J Immunol 183: 524–532.
36. Maldarelli F, Chen MY, Willey RL, Strebel K (1993) Human immunodeficiency virus type 1 Vpu protein is an oligomeric type I integral membrane protein. J Virol 67: 5056–5061.
37. Ozaki S, Kosaka M, Wakahara Y, Ozaki Y, Tsuchiya M, et al. (1999) Humanized anti-HM1.24 antibody mediates myeloma cell cytotoxicity that is enhanced by cytokine stimulation of effector cells. Blood 93: 3922–3930.
38. Ryo A, Tsurutani N, Ohba K, Kimura R, Komano J, et al. (2008) SOCS1 is an inducible host factor during HIV-1 infection and regulates the intracellular trafficking and stability of HIV-1 Gag. Proc Natl Acad Sci U S A 105: 294–299.

Follicular Dendritic Cells Activate HIV-1 Replication in Monocytes/Macrophages through a Juxtacrine Mechanism Mediated by P-Selectin Glycoprotein Ligand 1[1]

Kenji Ohba,*† Akihide Ryo,[2]* Md. Zahidunnabi Dewan,*†‡ Mayuko Nishi,* Toshio Naito,§ Xiaohua Qi,† Yoshio Inagaki,† Yoji Nagashima,¶ Yuetsu Tanaka,‖ Takashi Okamoto,# Kazuo Terashima,† and Naoki Yamamoto[2]*†

Follicular dendritic cells (FDCs) are located in the lymphoid follicles of secondary lymphoid tissues and play a pivotal role in the selection of memory B lymphocytes within the germinal center, a major site for HIV-1 infection. Germinal centers are composed of highly activated B cells, macrophages, CD4$^+$T cells, and FDCs. However, the physiological role of FDCs in HIV-1 replication remains largely unknown. We demonstrate in our current study that FDCs can efficiently activate HIV-1 replication in latently infected monocytic cells via an intercellular communication network mediated by the P-selectin/P-selectin glycoprotein ligand 1 (PSGL-1) interaction. Upon coculture with FDCs, HIV-1 replication was significantly induced in infected monocytic cell lines, primary monocytes, or macrophages. These cocultures were found to synergistically induce the expression of P-selectin in FDCs via NF-κB activation and its cognate receptor PSGL-1 in HIV-1-infected cells. Consistent with this observation, we find that this response is significantly blocked by antagonistic Abs against PSGL-1 and almost completely inhibited by PSGL-1 small interfering RNA. Moreover, a selective inhibitor for Syk, which is a downstream effector of PSGL-1, blocked HIV-1 replication in our cultures. We have thus elucidated a novel regulatory mechanism in which FDCs are a potent positive bystander that facilitates HIV-1 replication in adjacent infected monocytic cells via a juxtacrine signaling mechanism. *The Journal of Immunology,* **2009, 183: 524–532.**

The natural progression of HIV-1 infection consists of acute and chronic stages (1, 2). In the acute phase of viral infection, an initial peak level of plasma viremia appears within a couple of weeks of transmission. At this early time point in the course of infection, HIV-1 has disseminated to the lymphoid organs and viral reservoirs and latency have been established. The HIV-1 viral load stabilizes at a relatively low level after a period of acute viral infection, defined as the "set point," during which an immunological activation against HIV-1 is initiated. However, in tandem with seroconversion, HIV-1 production in reservoir or latently infected cells will eventually resume upon specific immunological responses such as host cytokine secretion or cell-mediated immune reactions (3–6).

Lymphoid organs have been proposed to function as a major reservoir for HIV-1 (7). During the course of HIV infection, T cells and macrophages in secondary lymphoid organs also become major reservoir cells for HIV-1 (8). Several in vitro studies have now identified potentially stable reservoirs of inducible latently infected CD4$^+$ cells carrying an integrated form of the viral genome (7–9). In addition to CD4$^+$ T cells, monocytes are thought to be major reservoirs for HIV-1 in vivo, since a number of blood monocytes are maintained in HIV-1-infected patients even during the late disease stages when T cells can be practically undetectable (10, 11). These observations suggest that infected CD4$^+$ T cells and macrophages provide sites as a stable reservoir and producer of HIV-1, causing the persistent production of progeny virus in lymphoid organs. However, it has not been well investigated how these reservoir cells can maintain sufficient levels of viral replication that will retain a sufficient viral load during the long course of this disease.

It is generally believed that the central point in the immune system is the lymphoid organs and germinal centers (GCs)[3] where several immune cell types are localized, although these circulate throughout the whole body (12–14). The GCs of secondary lymphoid tissues are composed of B cells, CD4$^+$ T cells, macrophages, and follicular dendritic cells (FDCs) (15–17). FDCs are characterized by the expression of CD21, CD35, CD40, and specific cell surface adhesion molecules including ICAM-1, VCAM-1, and the surface dendritic cell (DC) markers DC-SIGN and DRC-1 (16, 18–21). The FDCs play an important role in the

*AIDS Research Center, National Institute of Infectious Diseases, Toyama, Shinjyuku-ku, Tokyo, Japan; †Department of Molecular Virology, Graduate School of Medicine, Tokyo Medical and Dental University, Yushima, Bunkyo-ku, Tokyo, Japan; ‡Department of Pathology, New York University School of Medicine, New York, NY 10016; §Department of General Medicine, Juntendo University School of Medicine, Hongo, Bunkyo-ku, Tokyo, Japan; ¶Department of Pathology, Graduate School of Medicine, Yokohama City University, Fukuura, Kanazawa-ku, Kanagawa, Japan; ‖Department of Immunology, Graduate School of Medicine, University of the Ryukyus, Uehara, Okinawa, Japan; and #Department of Molecular and Cellular Biology, Nagoya City University Graduate School of Medical Sciences, Kawasumi, Mizuho-cho, Mizuho-ku, Nagoya, Aichi, Japan

Received for publication February 3, 2009. Accepted for publication April 25, 2009.

The costs of publication of this article were defrayed in part by the payment of page charges. This article must therefore be hereby marked *advertisement* in accordance with 18 U.S.C. Section 1734 solely to indicate this fact.

[1] This work was supported in part by grants from the Japanese Ministries of Education, Culture, Sports, Science and Technology (20390136, 13226027, 14406009, and 1941075) Health, Labour and Welfare (H18-005) and Human Health Science (H19-001) to N.Y. and A.R.

[2] Address correspondence and reprint requests to Dr. Akihide Ryo and Dr. Naoki Yamamoto, AIDS Research Center, National Institute of Infectious Diseases, 1-23-1 Toyama, Shinjyuku-ku, Tokyo 162-8640, Japan. E-mail addresses: aryo@nih.go.jp and nyama@nih.go.jp

[3] Abbreviations used in this paper: GC, germinal center; FDC, follicular dendritic cell; DC, dendritic cell; PSGL-1, P-selectin glycoprotein ligand 1; Syk, spleen tyrosine kinase; LTR, long terminal repeat; MOI, multiplicity of infection; siRNA, small interfering RNA.

www.jimmunol.org/cgi/doi/10.4049/jimmunol.0900371

immune response by interacting with $CD4^+$ T or B cells and in organization of the follicular structure.

In HIV infection, human FDCs can capture and retain infectious HIV particles in a stable manner on their cell surfaces for several months or even years via Fc receptors or other molecules (22–25). Unlike conventional DCs, FDCs are not themselves infected with HIV despite expression of chemokine receptors and DC-SIGN (24). Furthermore, active HIV infection is largely confined to sites surrounding the FDCs (24), suggesting that this microenvironment is highly conducive to infection with this virus. FDCs have also been shown to transmit signals to the GC microenvironment which also appears to increase HIV infection and replication (24, 25). Our previous study showed that FDCs stimulated virus production in MOLT-4 T cells preexposed to HIV-1(23). Very recently, Thacker et al. (26) also reported that FDCs contributed to virus replication in $CD4^+$ T cells infected with HIV-1 obtained from peripheral blood and GCs by increasing viral transcription mediated by TNF-α upon coculture. However, the role of FDCs in HIV-infected monocytes/macrophages is largely unknown.

We here report that FDCs can activate HIV-1 production in surrounding infected monocytes or macrophages via a cell-cell interaction with a clear mechanistic distinction from $CD4^+$ T cells reported by Thacker et al. (26). This enhancement in monocytic cells was found to be mediated mainly by an association between P-selectin on FDCs, acting as a ligand, and P-selectin glycoprotein ligand 1 (PSGL-1), the cognate receptor, on HIV-1-infected cells. Furthermore, we delineate the biological significance of the PSGL-1/spleen tyrosine kinase (Syk) pathway in the FDCs-mediated switch to induce HIV-1 replication. Our current findings thus shed new light on mechanisms involved in the HIV replication pathway that are mediated through intercellular communication and provide clues for the design of future novel therapeutic interventions against AIDS and related disorders.

Materials and Methods

Cell culture and reagents

Several FDC lines were established from fresh human palatine tonsils and maintained as described previously (23). Briefly, FDCs were isolated from fresh palatine tonsils surgically removed. Tonsils were cut into pieces in the thickness of 2–3 mm and then digested for 15 min at 37°C with collagenase (type I; Wako). Following rinsing with RPMI 1640 by centrifugation at 400 × *g* for 7 min, cells were filtered through at 70-μm nylon mesh and overlaid on a 1.25, 2.5, and 5% continuous BSA gradient at 1 × *g* for 2 h. The lowest fraction with a higher density fraction was resuspended and cultured in RPMI 1640 medium with 10% FCS. Cell clusters in the lowest fraction included cells positive for DRC-1, a specific maker of FDCs. One week after the culture, adherent spindle-shaped FDCs appeared from the cell clusters after having released lymphoid cells and spontaneously proliferated without additional cytokines or growth factors. The character of FDCs was checked with expression of FDCs makers such as CAN-42, S-100α, CD54, DC-SIGN, and CXCR4 on its surface. After culturing along more than 2 wk, FDCs were stocked in −80°C before use. PBMCs were separated from three healthy donors in accordance with the guidelines of the ethics committee of Tokyo Medical and Dental University. PBMCs were cultured in RPMI 1640 containing 10% FBS at 37°C in 5% CO_2. Primary monocytes were obtained from three healthy donors with Rosette Sep (StemCell Technologies) according to the manufacturer's instructions. Primary macrophages were differentiated from monocytes by culturing in RPMI 1640 containing 10% AB serum (Sigma-Aldrich) and 20 ng/ml M-CSF (R&D Systems) for 7 days. HIV-1 chronically infected monocytic cell line U1 cells (27) were cultured in RPMI 1640 supplemented with 10% FBS (Invitrogen Life Technologies). Coculturing and Transwell assays were performed using 1×10^5 HIV-infected cell lines or 2×10^5 primary cells with 1×10^4 FDCs. For the FDC supernatant assay, filtered (0.2 μm) supernatants from FDC cultures were collected and added to HIV-1-infected cells at a 1:4 volume supernatant:total volume of fluid ratio. In the cell fixation assay, FDCs incubated with 3% paraformaldehyde in PBS for 2 h were washed three times with PBS and then twice with RPMI 1640 before coculturing.

Virus preparation and infection

HIV-$1_{JR\text{-}FL}$ or HIV-$1_{NL4\text{-}3}$ viruses were generated by transfection of the pJR-FL or pNL4-3 construct in 293T cells, respectively. Virus preparations were passed through a 0.4-μm filter and titrated using a conventional method as described previously (28). For the HIV-1 infection of primary cells, PBMCs were infected with HIV-$1_{JR\text{-}FL}$ for 24 h following stimulation with PHA-P (3 μg/ml) for 3 days. To adjust the culture condition for monocytes/macrophages with that for PBMCs, monocytes or macrophages were also infected with HIV-$1_{JR\text{-}FL}$ for 24 h following stimulation with PHA-P (3 μg/ml) for 3 days. All primary cell cultures were maintained in the absence of IL-2. Jurkat or FDCs were infected with HIV-$1_{NL4\text{-}3}$ (multiplicity of infection (MOI) = 0.05) for 1, 3, or 5 days.

Antibodies

Polyclonal Abs raised against phospho-p65 (Ser^{536}), phospho-Syk (Tyr^{352}), phospho-IκBα (Ser^{32}), and unmodified Syk were purchased from Cell Signaling Technology. Anti-p65 polyclonal, actin, and PSGL-1 (KPL1) mAb were purchased from Santa Cruz Biotechnology. Anti-α-tubulin mAb was purchased from Sigma-Aldrich. Neutralizing Abs targeting PSGL-1 or ICAM-1 were purchased from R&D Systems. Anti-HIV-1 p24 mAb (2C2; mouse IgG1) was produced by Y. Tanaka (University of Ryukyus, Okinawa, Japan).

Isolation of total RNA from cells and quantitative RT-PCR

U1 cells and FDCs were harvested after coculturing and washed three times with PBS. Total RNA was then extracted using Isogen (Nippongene) according to the manufacturer's instructions. RNA (1 μg) was reverse transcribed using Superscript III (Invitrogen) before semiquantitative RT-PCR, and quantitative RT-PCR was performed using a SYBER Green One-step Real-time PCR kit (Invitrogen) with mRNA-specific primer pairs. Analyzed genes and corresponding primers are listed in supplemental Table I.[4]

Neutralization assay

HIV-1-infected cells were pretreated with neutralizing Abs (anti-PSGL-1, anti-ICAM-1, or control mouse IgG) for 2 h before and during coculturing. Optimal concentrations were determined by the IC_{50} values in accordance with the manufacturer's instructions. Culture supernatants were collected after 3 days and subjected to measurement of HIV-1 p24.

Chemicals and inhibitory assays

BAY11-7082 and JNK inhibitor II were purchased from Merck. The Syk-specific inhibitor ER-27319 (29, 30) was purchased from Sigma-Aldrich. Cells were pretreated with 30 μM ER-27319, 1 μM JNK inhibitor II, 1–2 μM BAY11-7082, or DMSO (Sigma-Aldrich) for 2 h. The inhibitor treated/untreated cells were then cocultured with FDCs in the presence of Syk or NF-κB inhibitor. In small interfering RNA (siRNA) experiments, U1 cells were transfected with control or PSGL-1 siRNA (Santa Cruz Biotechnology) by Nucleofector (Amaxa) and then cocultured with FDCs. Lysates and supernatants were collected from these cultures after 3 days for measurement of p24 and Western blotting analysis.

Flow cytometry

Cells were washed twice with staining buffer (3% FBS and 0.09% NaN_3/PBS) and then stained with PSGL-1-RP-E (BD Biosciences) for 30 min on ice. Cells were then washed twice and processed for flow cytometry.

Measurement of HIV-1 p24

Cell culture supernatants were collected after centrifugation at 4000 rpm for 5 min at 4°C and then processed for measurement of HIV-1 p24 by using Lumipulse (Fujirebio) according to the manufacturer's instructions. Assays were performed in triplicate.

Results

FDCs activate HIV-1 production in adjacent HIV-1-infected monocytic cells

To address whether FDCs can also activate HIV-1 replication in the surrounding infected monocytes/macrophages as an effective bystander or stimulator, several primary FDCs were established from fresh palatine tonsils of three healthy human donors (23).

[4] The online version of this article contains supplemental material.

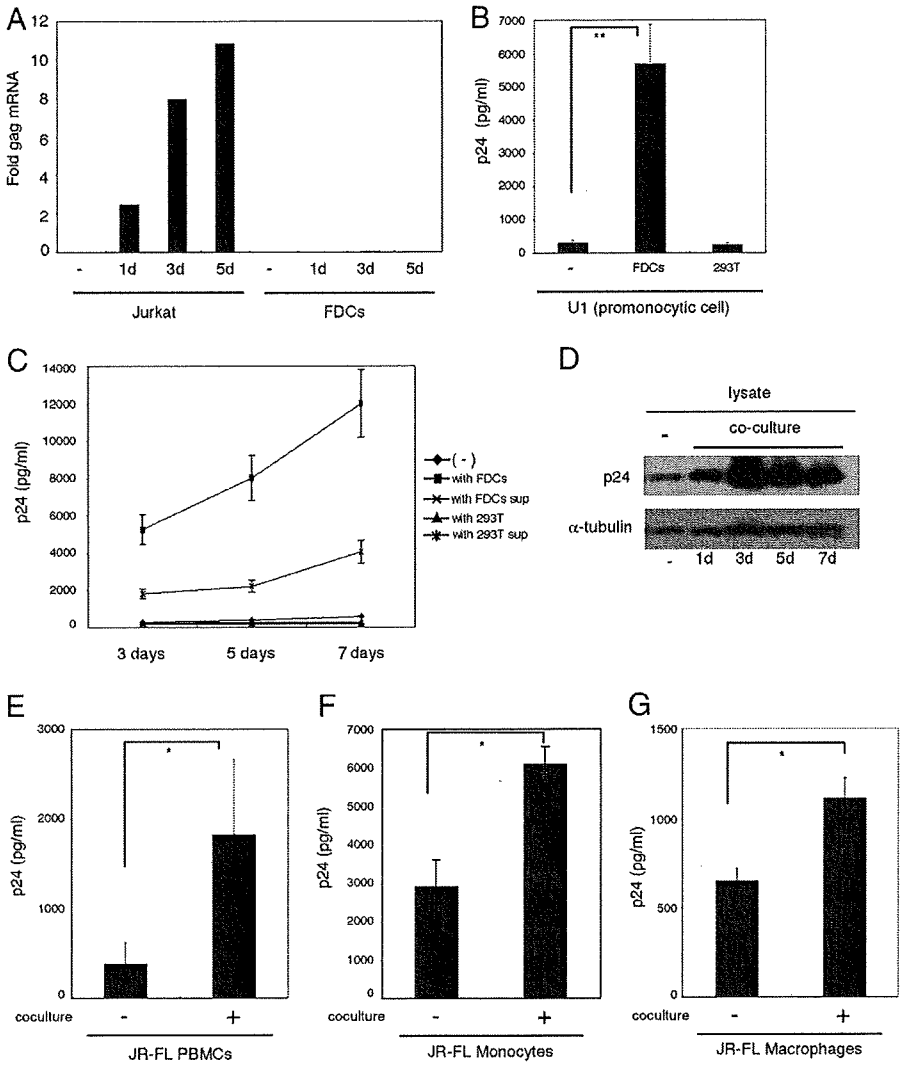

FIGURE 1. FDCs activate HIV-1 production in adjacent HIV-1-infected cells. *A*, Jurkat or FDCs were infected with HIV-1_{NL4-3} (MOI = 0.05) for 1, 3, or 5 days. Cells were collected and then lysed for the separation of total RNA. Total RNA were treated with DNase I followed by quantitative RT-PCR with specific primer sets for either HIV-1 Gag or G3PDH. The data shown are the fold inductions normalized by G3PDH. *B*, U1 cells (1×10^5 cells/well) were cultured alone or in coculture with either FDCs or 293T cells (1×10^4 cells/well) for 3 days. Cell supernatants were then collected and assayed for measurement of p24. *C*, p24 levels in culture supernatants were monitored at 3, 5, and 7 days. *D*, p24 levels in lysates were monitored at 1, 3, 5, and 7 days by Western blot. *E*, PBMCs separated from a healthy donor were cultured with 3 μg/ml PHA for 3 days followed by infection with HIV-1_{JR-FL} (MOI = 0.05) for 24 h. The PBMCs (2×10^5 cells/well) were then cocultured with FDCs (1×10^4 cells/well) in the absence of IL-2 for 14 days. Culture supernatants were then assayed for measurement of p24. *F*, Monocytes separated from a healthy donor were cultured with 3 μg/ml PHA for 3 days followed by infection with HIV-1_{JR-FL} (MOI = 0.05) for 24 h. The monocytes (1×10^5 cells/well) were then cocultured with FDCs (1×10^4 cells/well) for 14 days. *G*, Primary differentiated macrophages were cultured with 3 μg/ml PHA for 3 days followed by infection with HIV-1_{JR-FL} (MOI = 0.05) for 24 h. The macrophages (1×10^5 cells/well) were then cocultured with FDCs (1×10^4 cells/well) for 7 days. Culture supernatants were then assayed for measurement of p24. The data shown in *B* are the average ± SD of at least three independent experiments. The data presented in *E–G* were obtained using samples of three donors (*, $p \leq 0.05$ and **, $p \leq 0.01$ by the Student t test).

Since each of these established cell lines was very similar in nature, exhibiting typical properties of FDCs (positive for CAN-42, S-100α, CD54, DC-SIGN, and CXCR4; morphological character such as spine-like spiculae and intercellular gap junction), the FDC 1 line was mainly used in subsequent experiments. FDCs themselves were not productively infected with HIV-1 (Fig. 1*A*), consistent with previous reports (22–25).

Initially, the FDCs were cocultured with chronically HIV-1-infected monocytic cell line U1 to examine whether they had the ability to activate HIV-1 replication. After 3 days of growth, HIV-1 production was analyzed for HIV-1 p24. The results showed that coculturing with FDCs significantly induced HIV-1 replication in the two infected cell types tested, whereas no such induction was observed when the U1 cells were cultured with 293T cells (Fig. 1*B*). A parallel kinetic study further demonstrated that the p24 levels in supernatants and lysates were increased in a time-dependent manner in U1 cells grown under these coculture conditions (Fig. 1, *C* and *D*). To address whether this trend occurred also in primary cells, FDCs were cocultured with PBMCs from healthy donors after infection with R5 (HIV-1_{JR-FL}) virus. As shown in Fig. 1*E*, the virus production was considerably augmented in coculture with FDCs. Furthermore, parallel experiments revealed that the virus production in monocytes or macrophages purified from PBMCs was also increased by coculturing with

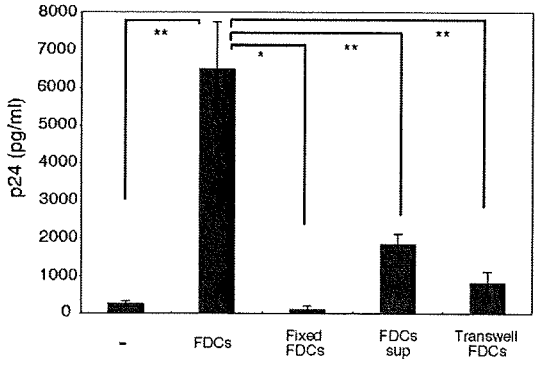

FIGURE 2. The enhancement of HIV-1 production by FDCs requires direct cell-cell interactions. U1 cells (1×10^5 cells/well) were cocultured with regular or paraformaldehyde-fixed FDCs (1×10^4 cells/well), cultured separately with FDCs on Transwell plates, or grown in medium supplemented with FDC culture supernatant at a 1:4 ratio of volume supernatant:total volume of fluid. Cell supernatants were collected after 3 days and assayed for measurement of p24. The data shown are the average ± SD of two independent experiments (*, $p \leq 0.05$ and **, $p \leq 0.01$ by the Student t test).

FDCs (Fig. 1, *F* and *G*). These data thus strongly indicate that FDCs can indeed activate viral replication monocytes/macrophages infected with HIV-1.

The enhancement of HIV-1 production by FDCs requires direct cell-cell interactions

To investigate whether this stimulation by FDCs was achieved by direct cell-cell interaction or soluble factors, we used two different cell culture methods for FDCs and U1 cells as follows: 1) FDCs were separately cultured with U1 cells using Transwells and 2) U1 cells were grown in culture medium supplemented with FDC supernatant. Although both culture systems could partially induce HIV-1 replication in U1 cells, these effects were ~20–30% of the full induction of those observed following coculture with FDCs (Fig. 2). This suggested that direct cell-cell interactions might be required for the full induction of HIV-1 replication in monocytic cells, although certain soluble factors may also activate HIV-1 replication to a lesser degree. Furthermore, the fixation of FDCs with paraformaldehyde before coculture completely abrogated the induction of HIV-1 replication in U1 cells, suggesting a requirement for bioactive cell surface molecules in this response.

Taken together, these data indicate that direct interactions via cell surface bioactive molecules are important to fully stimulate HIV-1 replication in monocytic U1 cells by FDCs.

Activation of NF-κB in both FDCs and HIV-1-infected cells following coculture

Our initial analysis demonstrated that FDCs can enhance HIV-1 replication in infected cells via cell-cell interaction. We thus examined whether this induction is initiated by the activation of the HIV-1 long-terminal repeat sequence (LTR). Quantitative and semiquantitative RT-PCR analyses revealed that the levels of HIV-1 mRNA were increased in U1 cells in tandem with increased supernatant p24 levels under coculture conditions with FDCs (Fig. 3, *A* and *B*).

HIV-1 replication has been shown to be regulated by host transcription factors such as NF-κB, NF-AT, Sp1, and AP-1 that are

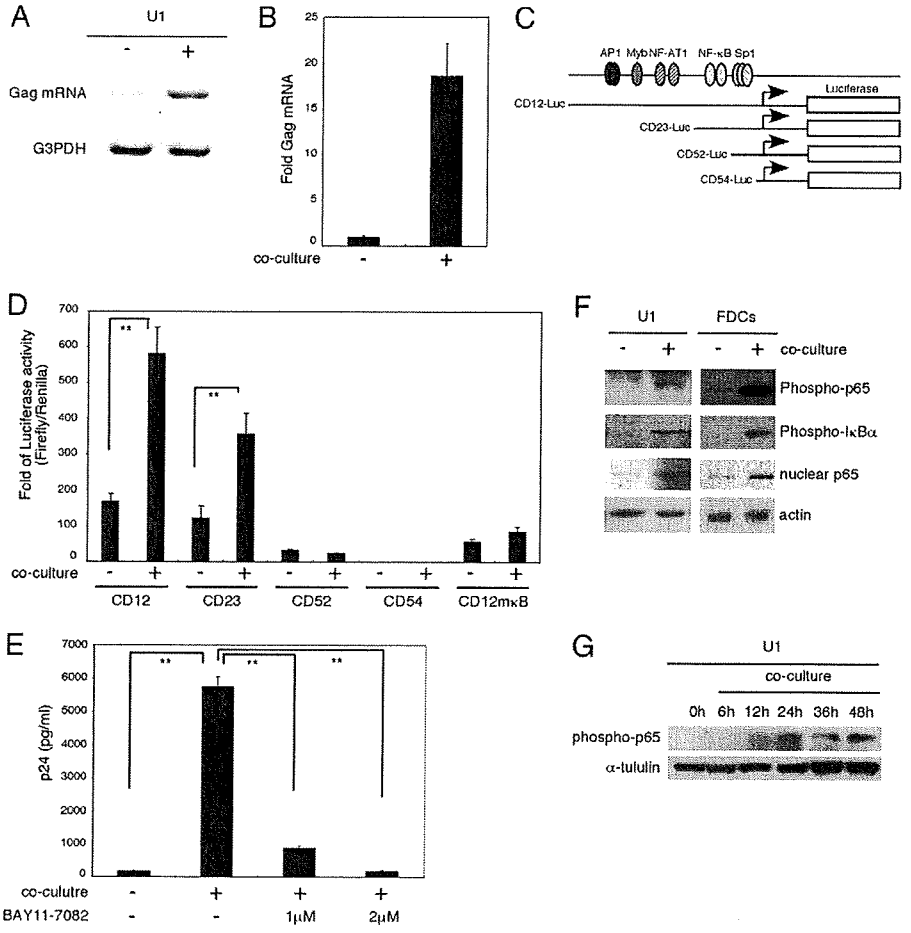

FIGURE 3. Activation of NF-κB in both FDCs and HIV-1-infected cells. *A* and *B*, U1 cells (1×10^5 cells/well) were cocultured with FDCs (1×10^4 cells/well) for 5 days and the mRNA levels for the indicated genes were measured by RT-PCR (*A*) or quantitative RT-PCR (*B*). *C*, Schematic representation of HIV-1 LTR-derived luciferase reporter constructs. *D*, U1 cells (1×10^5 cells/well) were initially transfected with the indicated reporter constructs and then cocultured with FDCs (1×10^4 cells/well) for 48 h, which was followed by a gene reporter assay. *E*, U1 cells (1×10^5 cells/well) were pretreated with the indicated concentrations of BAY 11-7082 for 2 h and then cocultured with FDCs (1×10^4 cells/well) for 3 days in the presence of the same concentration of BAY 11-7082. Cell supernatants were then collected and assayed for measurement of p24. *F*, U1 cells (1×10^5 cells/well) were cocultured with FDCs (1×10^4 cells/well) for 3 days and both cell types were collected and subjected to immunoblotting analysis for phospho-p65 (Ser^{536}), phospho-IκBα (Ser^{32}), p65, or actin. *G*, U1 cells (1×10^5 cells/well) were cocultured with FDCs (1×10^4 cells/well) and collected at the indicated time points. Cell lysates were subjected to immunoblot analysis using either phospho-p65 (Ser^{536}) or α-tubulin Abs. The data shown are the average ± SD of three independent experiments (*, $p \leq 0.05$ and **, $p \leq 0.01$ by the Student t test).